

Chapter 2

Description of IUE Data

2.1 Raw Image Data and Label Parameters

Each raw *IUE* image consists of a 768×768 array of 8-bit picture elements or “pixels”. Partial-read images, which are not full 768×768 images, are discussed in Chapter 4.3. Each vidicon scan line consists of 768 pixels or “samples” obtained in minor frame units of 96 pixels; 768 such scan lines compose the entire image. Line 1, sample 1 is at the upper left corner of the image; line 768, sample 768 is at the lower right corner of the image. Each raw pixel value lies in the range 0 to 255 (integers only). The units of raw pixel values are data numbers (DN), which are proportional (up to the telemetry system limit of 255) to the integrated charge read out from the SEC Vidicon target in the camera scanning process. Since the telemetry system saturates at 255, the DN/charge proportionality breaks down at that level.

Associated with each raw image is a set of 20 header, or label, records. Each record is 360 8-bit bytes long and is a concatenation of five 72-byte logical records. This set of 20 label records was generated by the *IUE* Operations Control Center (IUEOCC) software during image acquisition and contains various identifying parameters and scientific/engineering data pertinent to the image.

Raw *IUE* images must be corrected for the instrumental effects of the SEC Vidicon camera system before quantitatively meaningful data can be extracted from them. The correction for radiometric (photometric) non-linearities and non-uniformities is discussed in Chapter 6. The removal of geometric distortions introduced by the vidicon system are described in Chapter 7. The layout of the spectral format in either dispersion mode is mathematically set forth by the methods related in Chapter 8. Figures 2.1 through 2.15 illustrate schematically the spectral formats in both dispersion modes, for both apertures, for all three operational cameras and refer to raw image space. The square border defines the 768×768 array comprising the whole image, whereas the inscribed arcs roughly define the target ring, which is the area within which the photometric correction is applied (Chapter 6) and from which spectral information is extracted. For high dispersion, the extracted odd and even echelle orders are shown in separate figures. Numbers and tick marks mark the

wavelengths in Ångstroms.

2.2 Spectrograph Geometry

Both the long- and short-wavelength *IUE* spectrographs have two entrance apertures: a small aperture (nominal 3 arcsec diameter circle) and a large aperture (nominal 10 arcsec by 20 arcsec slot). Although the various methods available for determining the fundamental dimensions do not always yield results which agree to within the limits set by the internal consistency of each (see Panek 1982), the *IUE* Three Agency Committee adopted recommended values for certain dimensions, which are presented in Table 2.1. These values do not reflect the true physical dimensions of the apertures but rather the size as projected on the camera faceplate. As a result, each spectrograph has its own distinct measurement of aperture sizes. Accurate measurements of the trail lengths are necessary, as such information

Table 2.1: Officially Adopted Dimensions for the Apertures in Each Spectrograph, Measured on LWP, LWR, and SWP Images

| Dimension | LWP | SWP | LWR |
|--|--------------|-------------|-------------|
| Major Axis Trail Length (<i>arcsec</i>) | 21.84±0.39 | 21.48±0.39 | 22.55±0.62 |
| Large-Aperture Length (<i>arcsec</i>) | 22.51±0.40 | 21.65±0.39 | 23.24±0.64 |
| Minor Axis Trail Length (<i>arcsec</i>) | 10.21±0.18 | 9.24±0.11 | 9.88±0.42 |
| Large-Aperture Width (<i>arcsec</i>) | 9.91±0.17 | 9.07±0.11 | 9.59±0.41 |
| Large-Aperture Area (<i>arcsec</i> ²) | 218.17±10.12 | 215.33±6.55 | 209.29±9.25 |
| Small-Aperture Area (<i>arcsec</i> ²) | 6.78±0.97 | 6.72±0.96 | 6.31±0.75 |

is used to calculate exposure times for trailed images. In addition, knowledge of the effective aperture area is needed to calibrate properly spectra of extended objects.

The camera plate scales have been redetermined (Garhart 1996; LWP 1.5644, LWR 1.5526, and SWP 1.5300 arcseconds per pixel) using the most recent measurements for the small-to-large aperture offsets in pixels (Table 2.2) and FES aperture center locations in arcseconds (Pitts 1988). These latest incarnations replace the oft-quoted plate scale figure of 1.525 arcseconds per pixel (Bohlin et al. 1980), a value that had been used for all three cameras. The aperture separations in the directions along and perpendicular to the dispersion are given in Table 2.2 for low dispersion. The corresponding values for the high-dispersion offsets are obtained by transposing the entries for the low-dispersion offsets along and perpendicular to the dispersion in Table 2.2. Refer to Figures 2.16 through 2.18 to determine the correct sign for the high-dispersion offsets. These values are defined in a geometrically corrected frame of reference. The total offset is defined as the square root of the sum of the squares of the individual terms. In low dispersion, the offsets along the dispersion

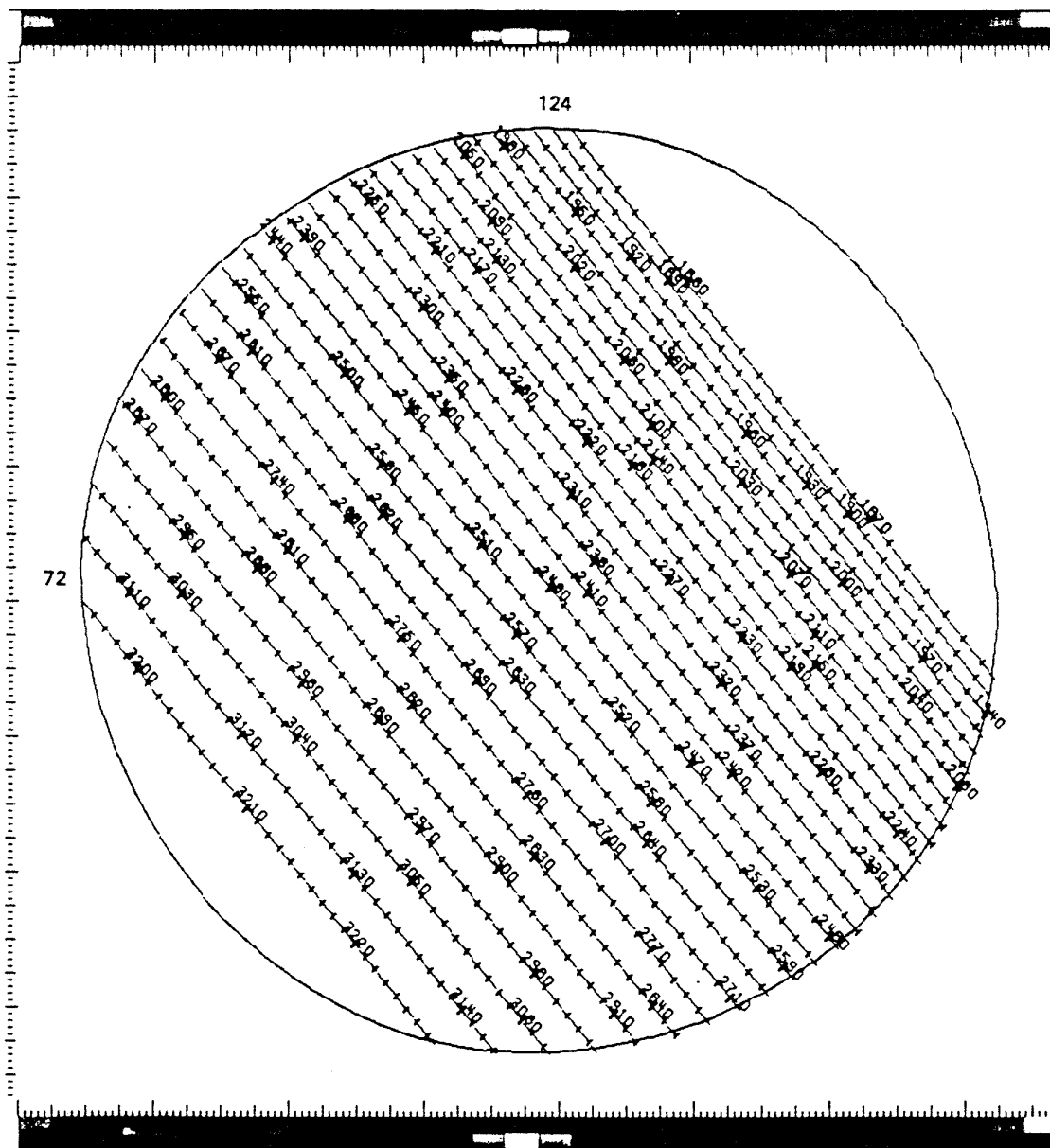


Figure 2.1: LWP small-aperture high-dispersion (even orders) format.

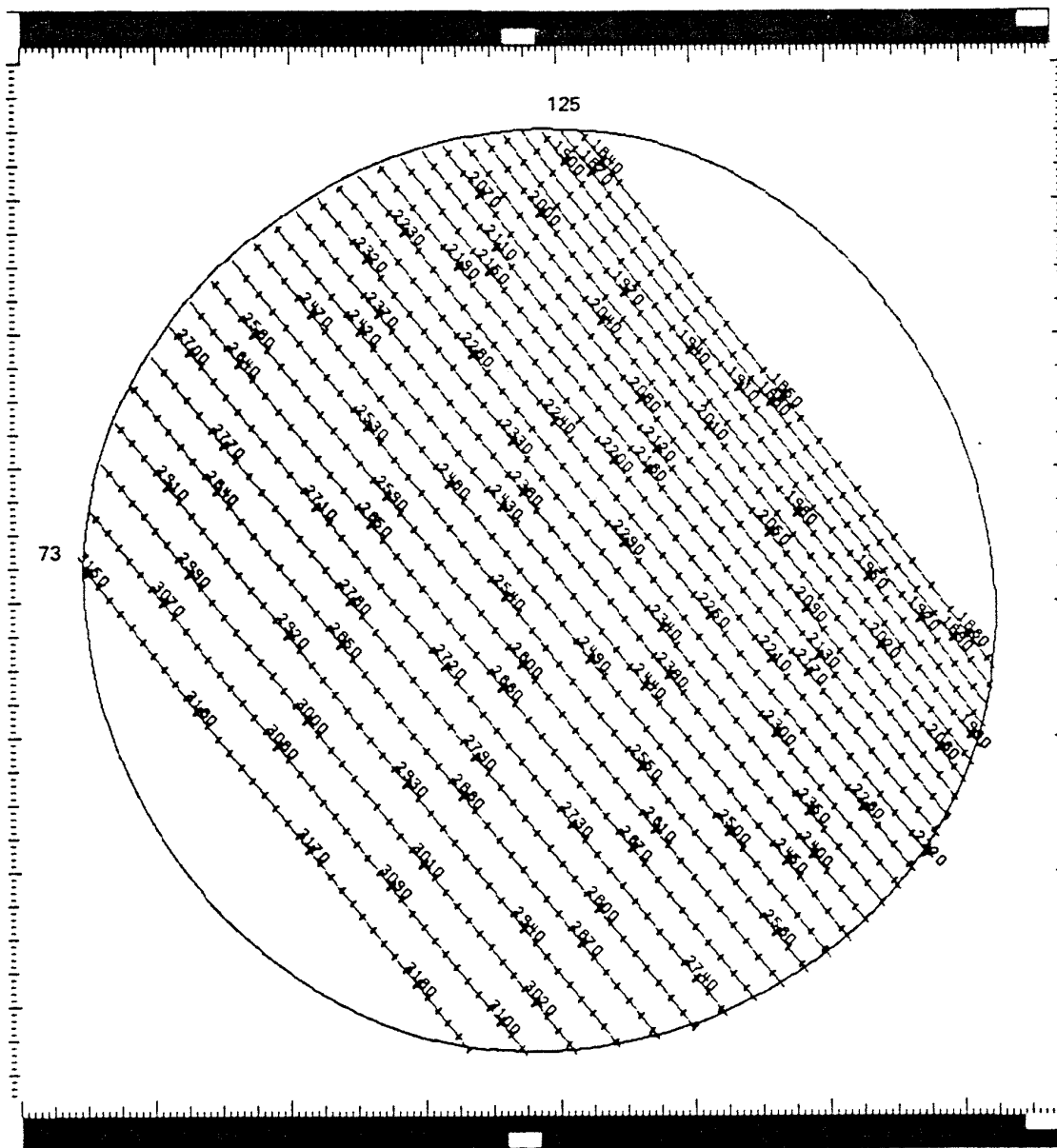


Figure 2.2: LWP small-aperture high-dispersion (odd orders) format.

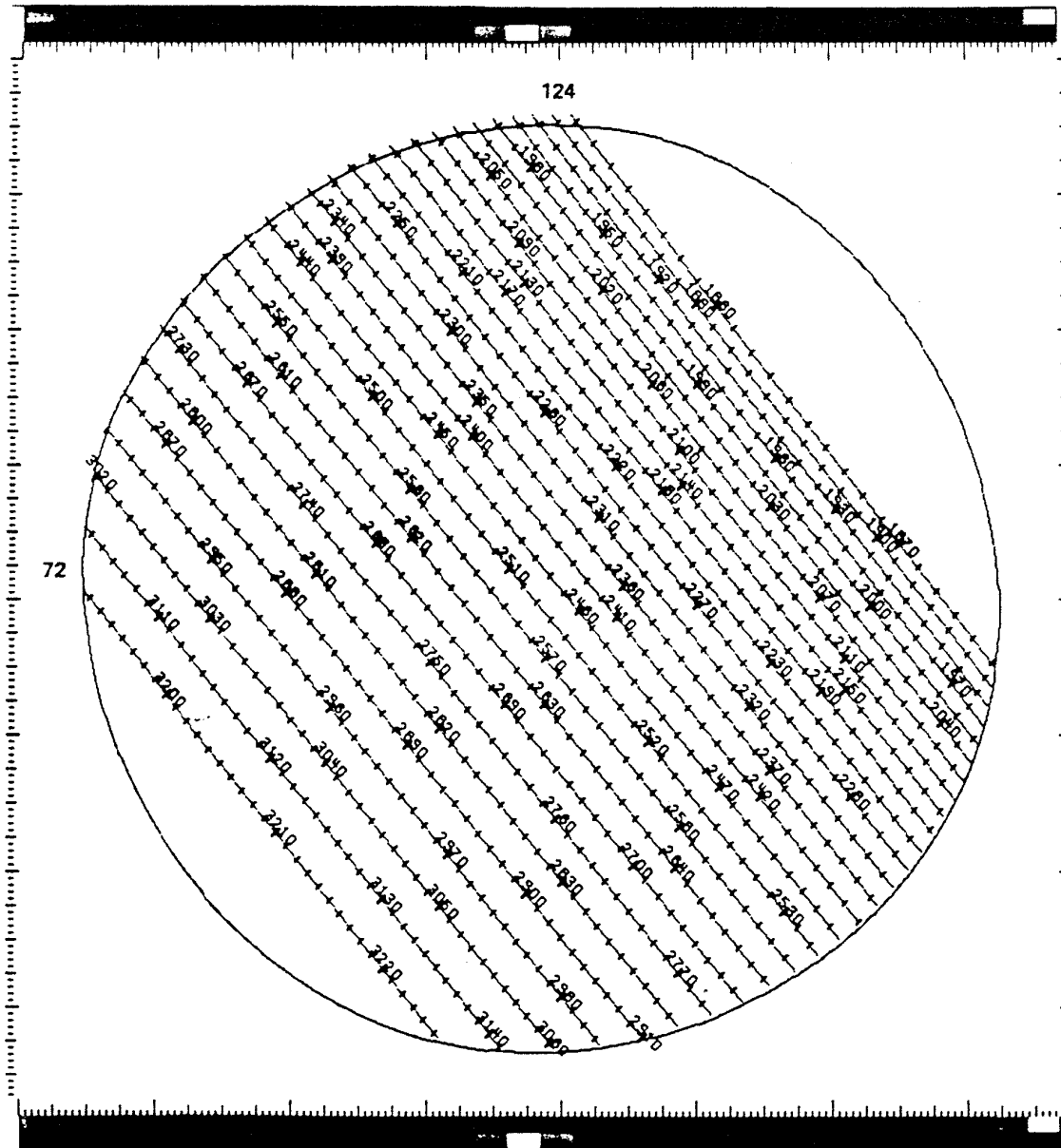


Figure 2.3: LWP large-aperture high-dispersion (even orders) format.

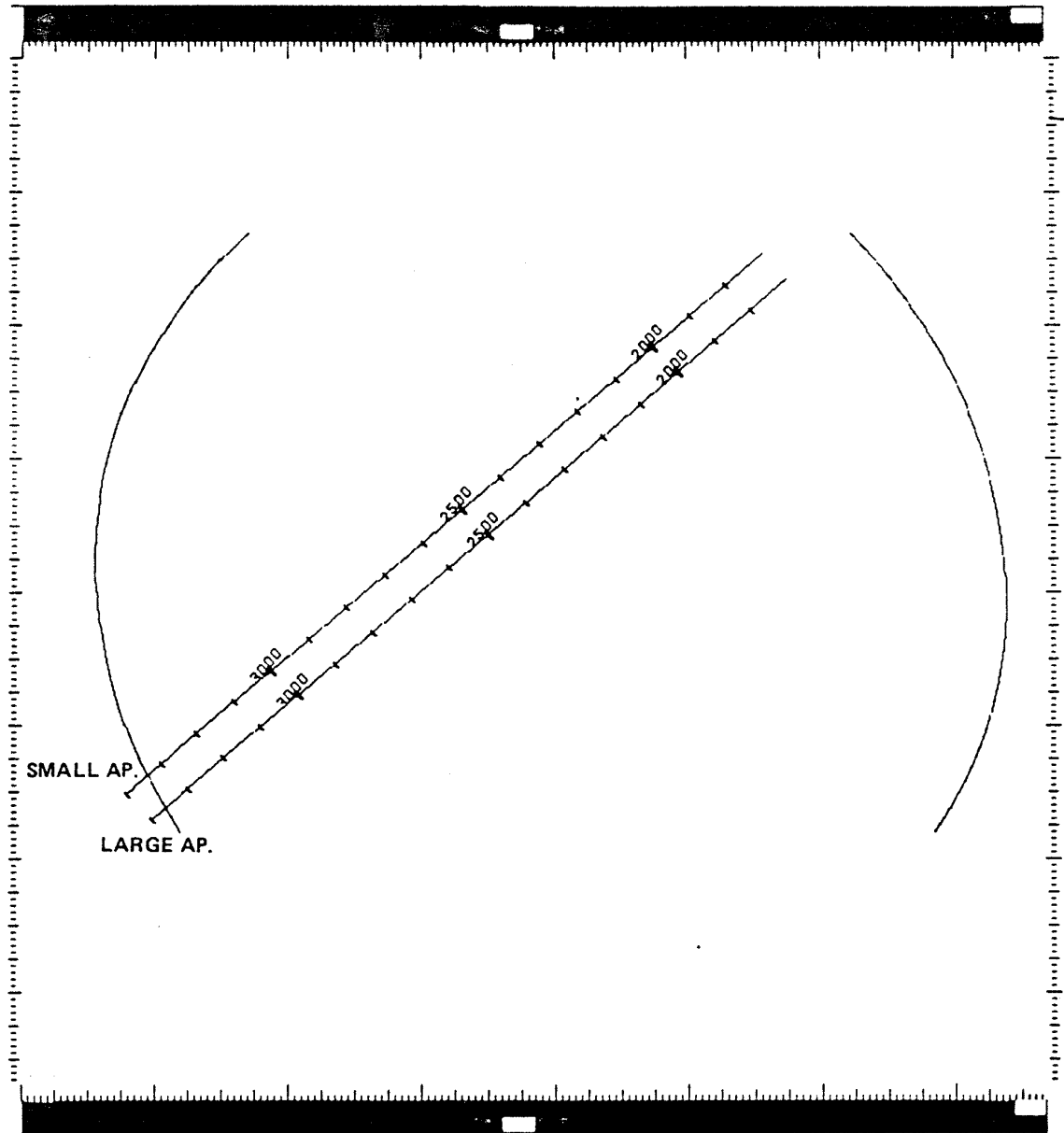


Figure 2.5: LWP large- and small-aperture low-dispersion format.

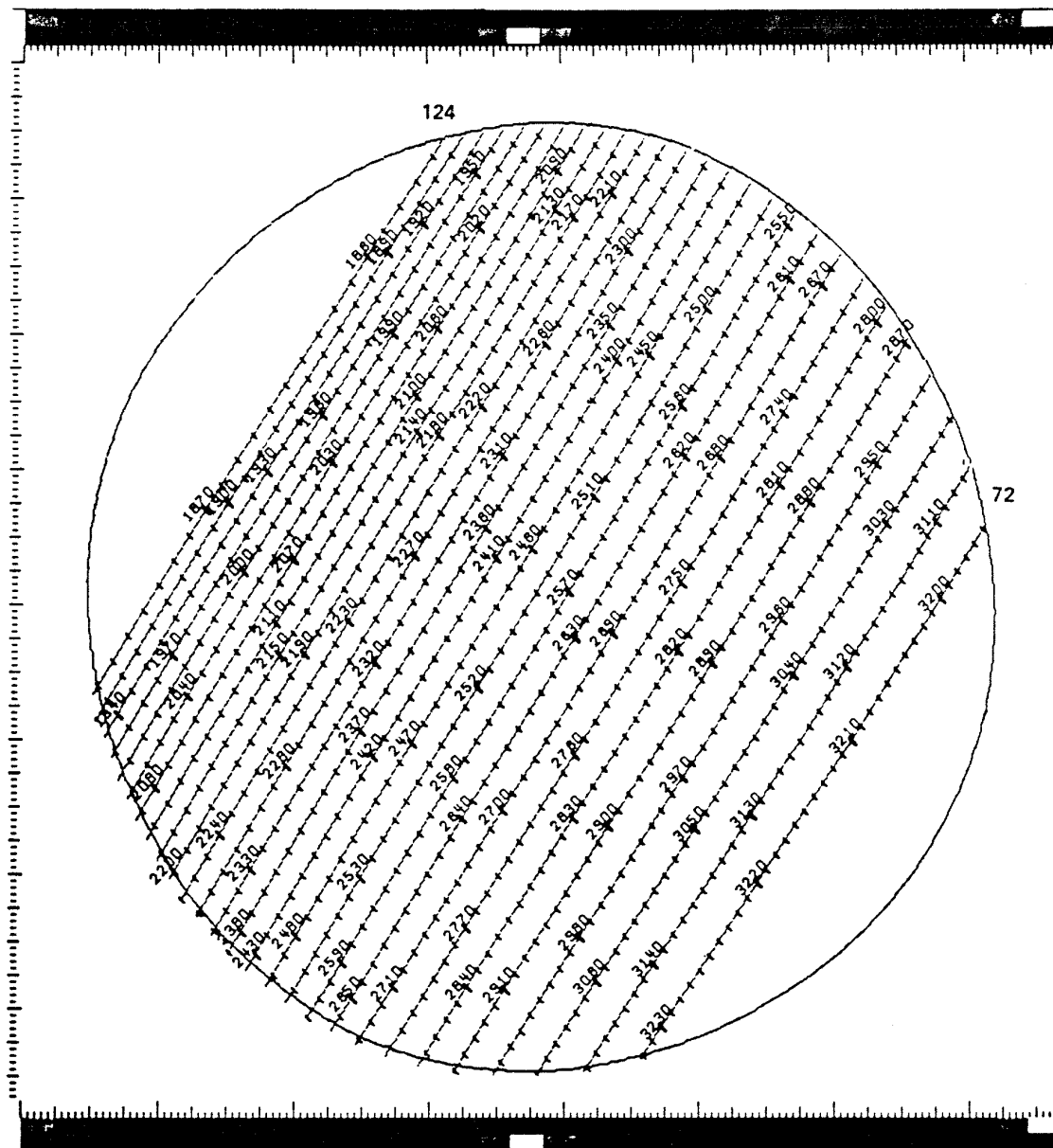


Figure 2.6: LWR small-aperture high-dispersion (even orders) format.

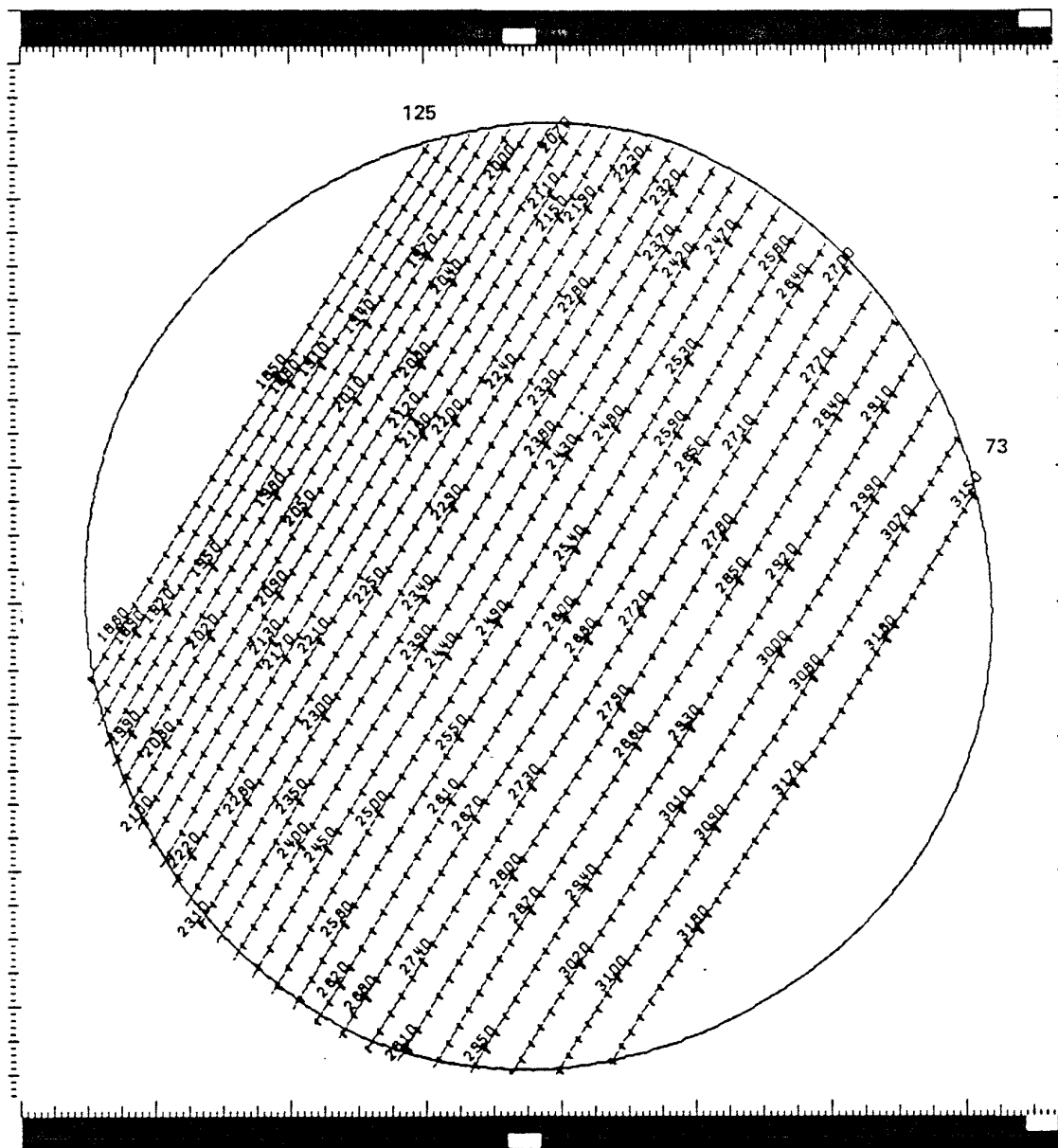


Figure 2.7: LWR small-aperture high-dispersion (odd orders) format.

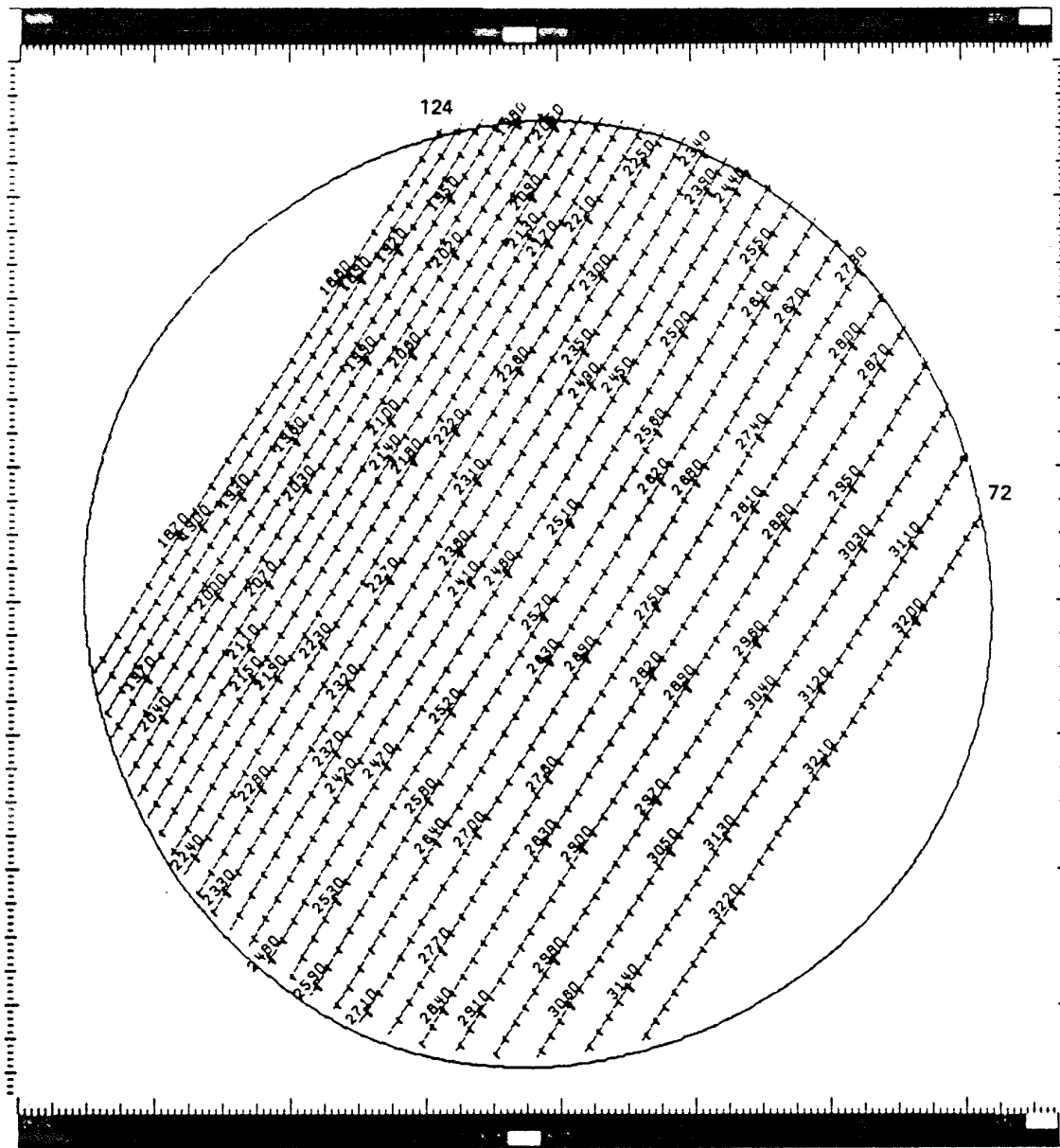


Figure 2.8: LWR large-aperture high-dispersion (even orders) format.

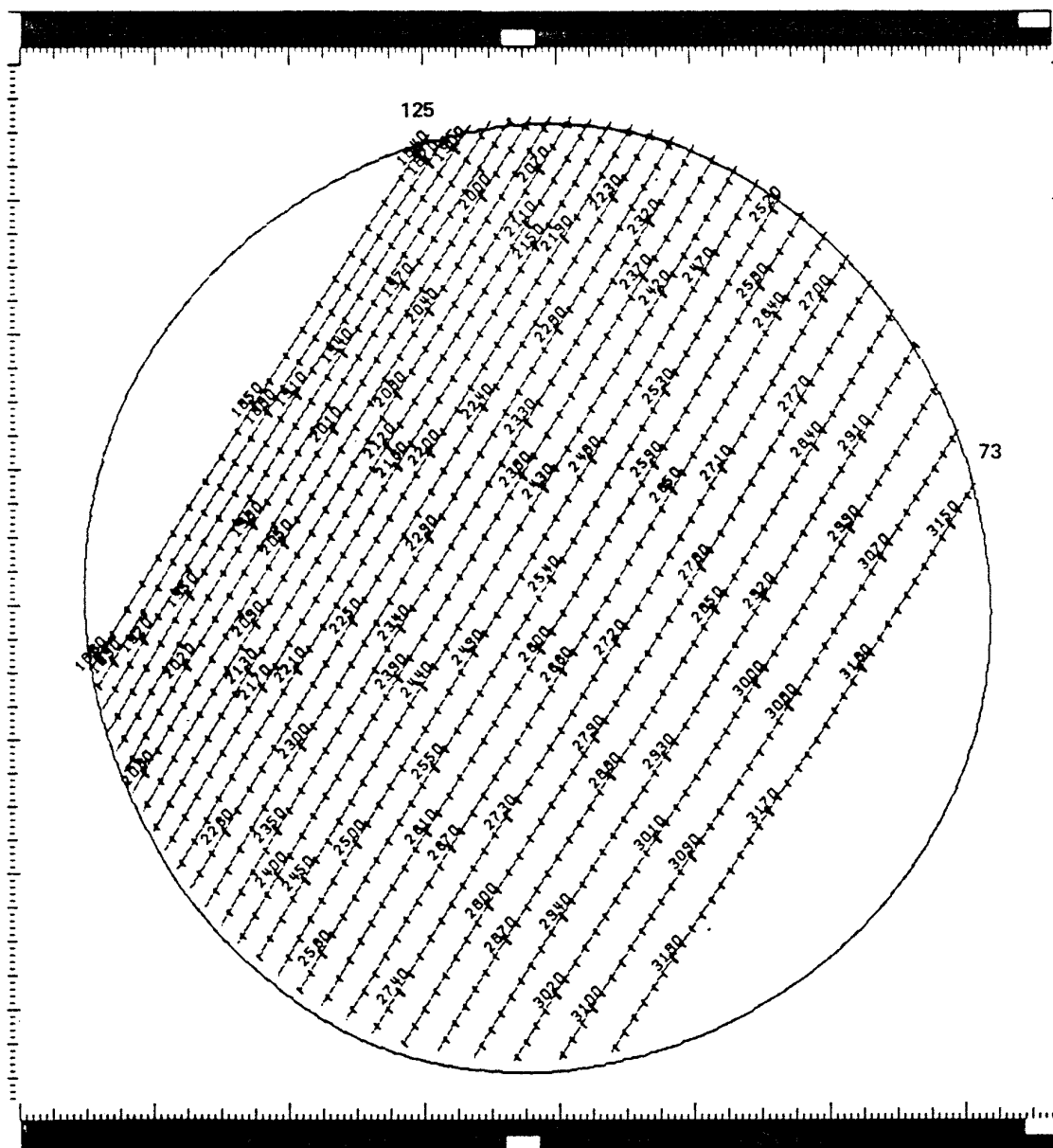


Figure 2.9: LWR large-aperture high-dispersion (odd orders) format.

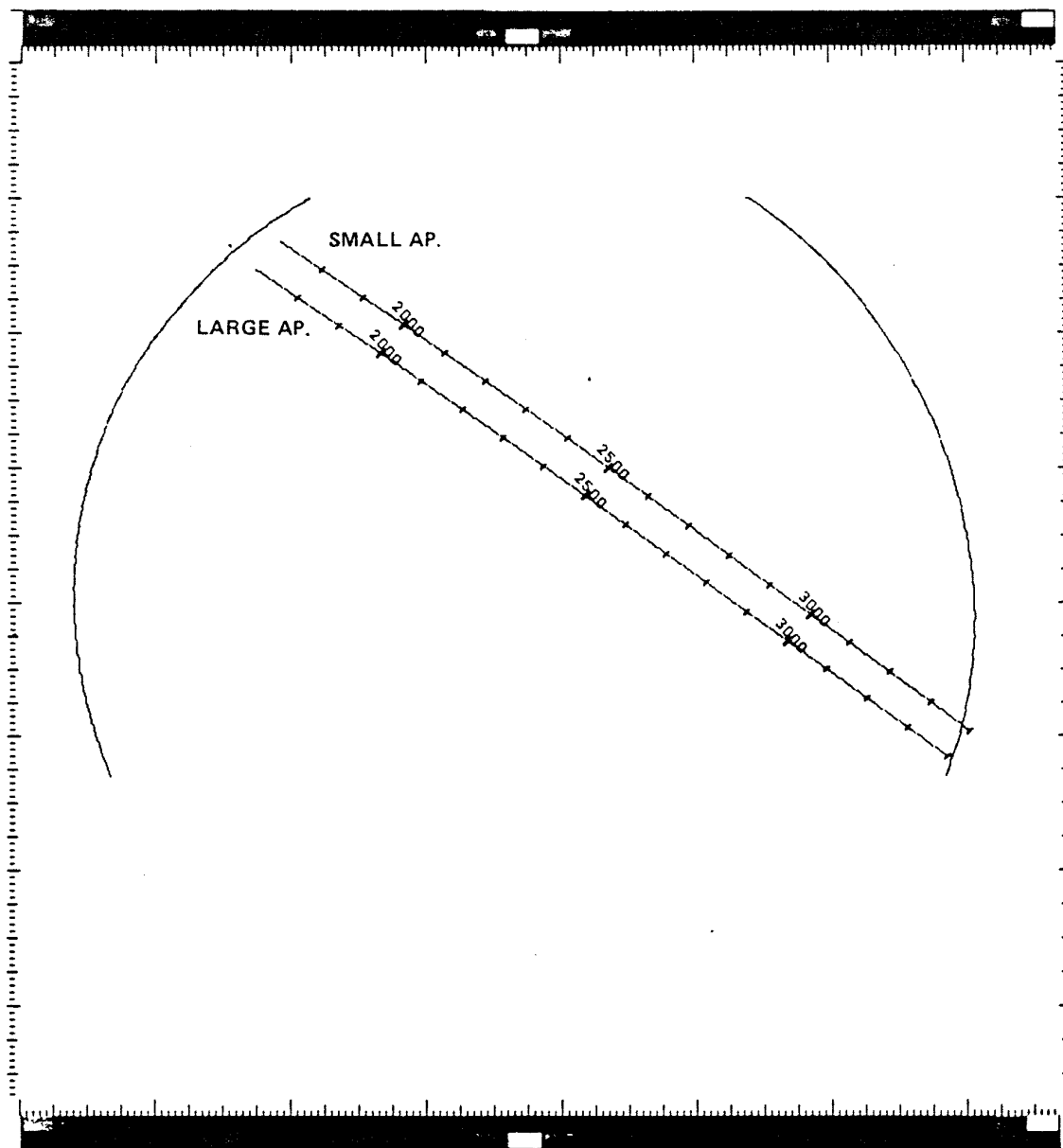


Figure 2.10: LWR large- and small-aperture low-dispersion format.

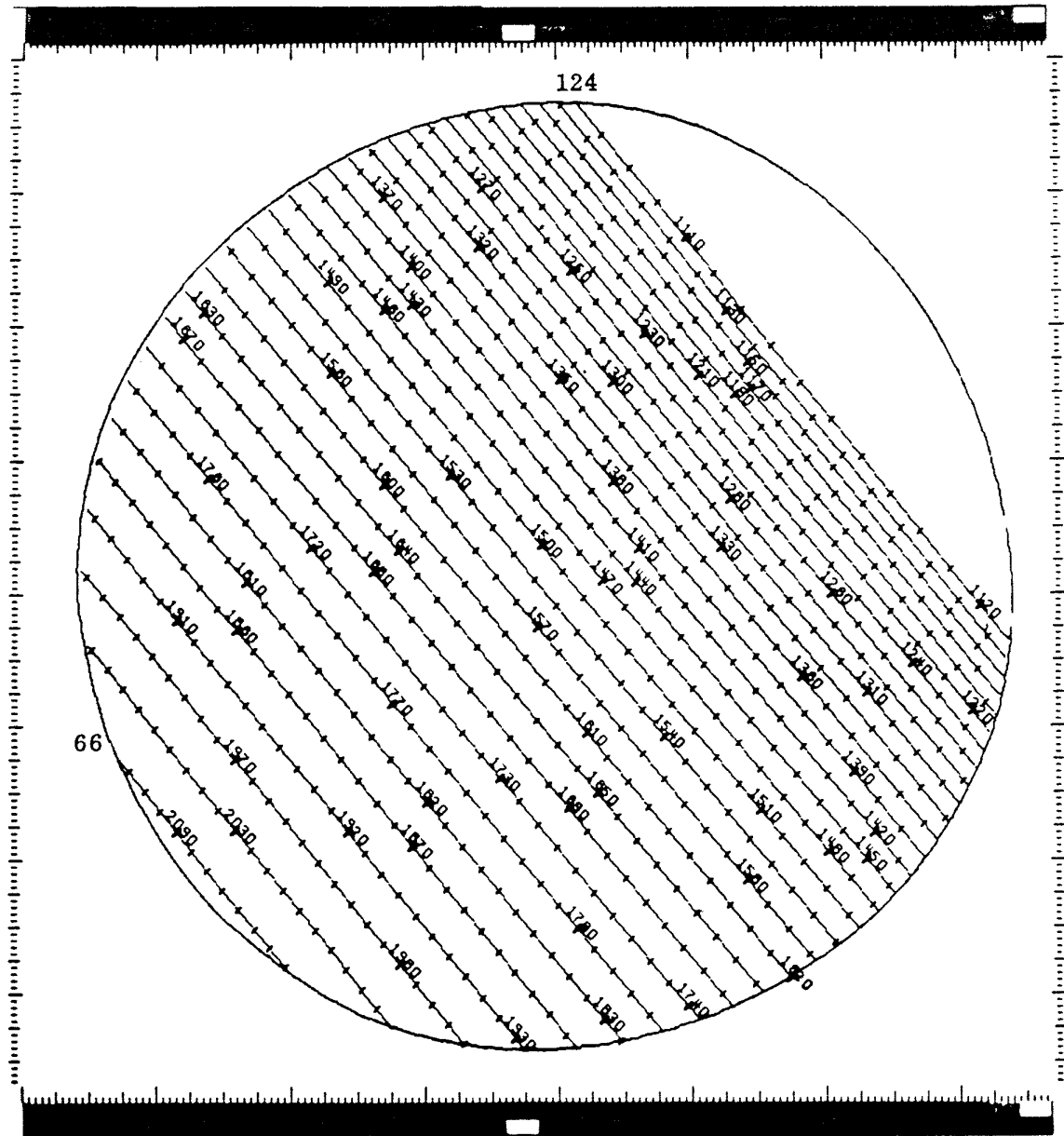


Figure 2.11: SWP small-aperture high-dispersion (even orders) format.

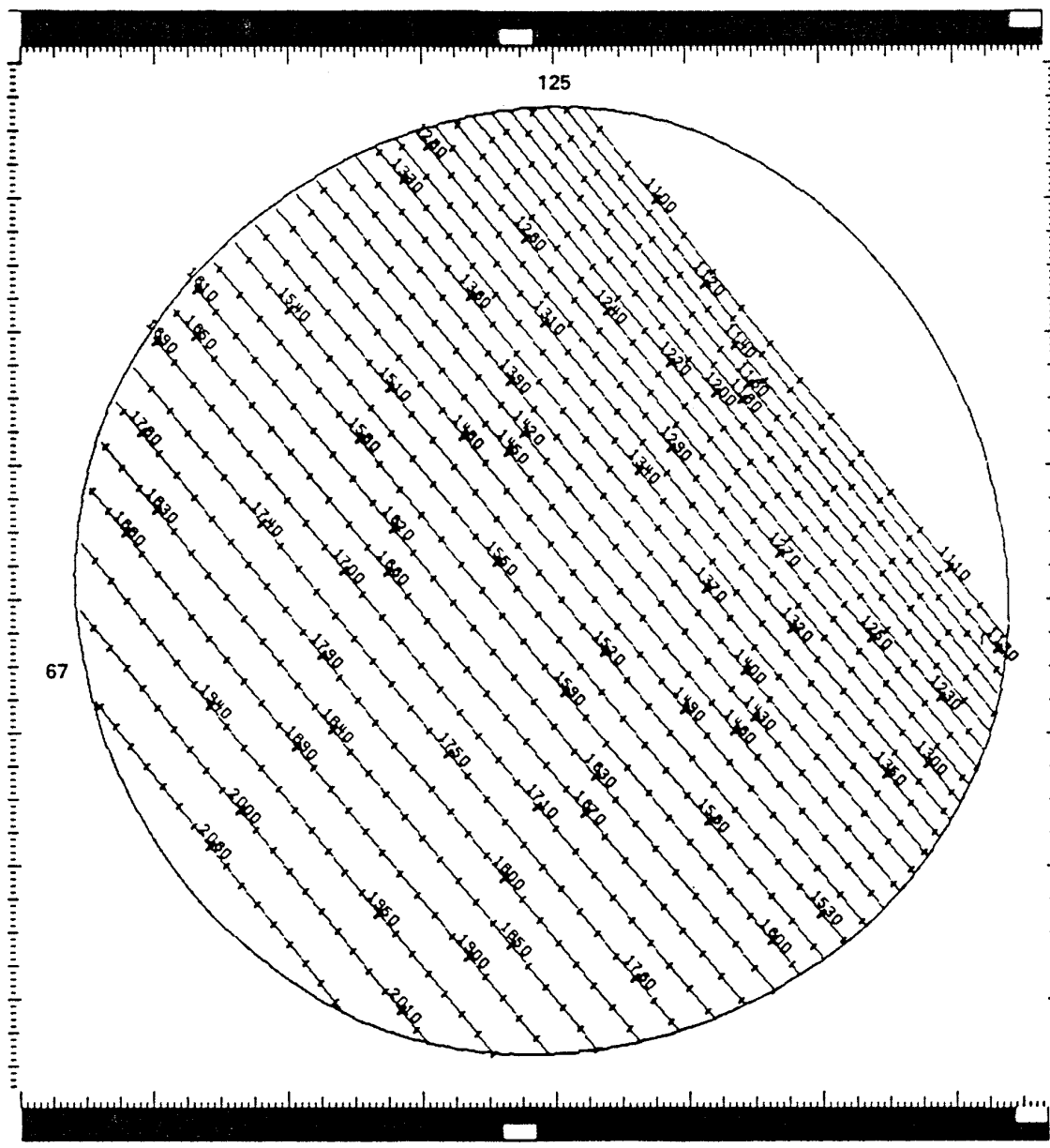


Figure 2.12: SWP small-aperture high-dispersion (odd orders) format.

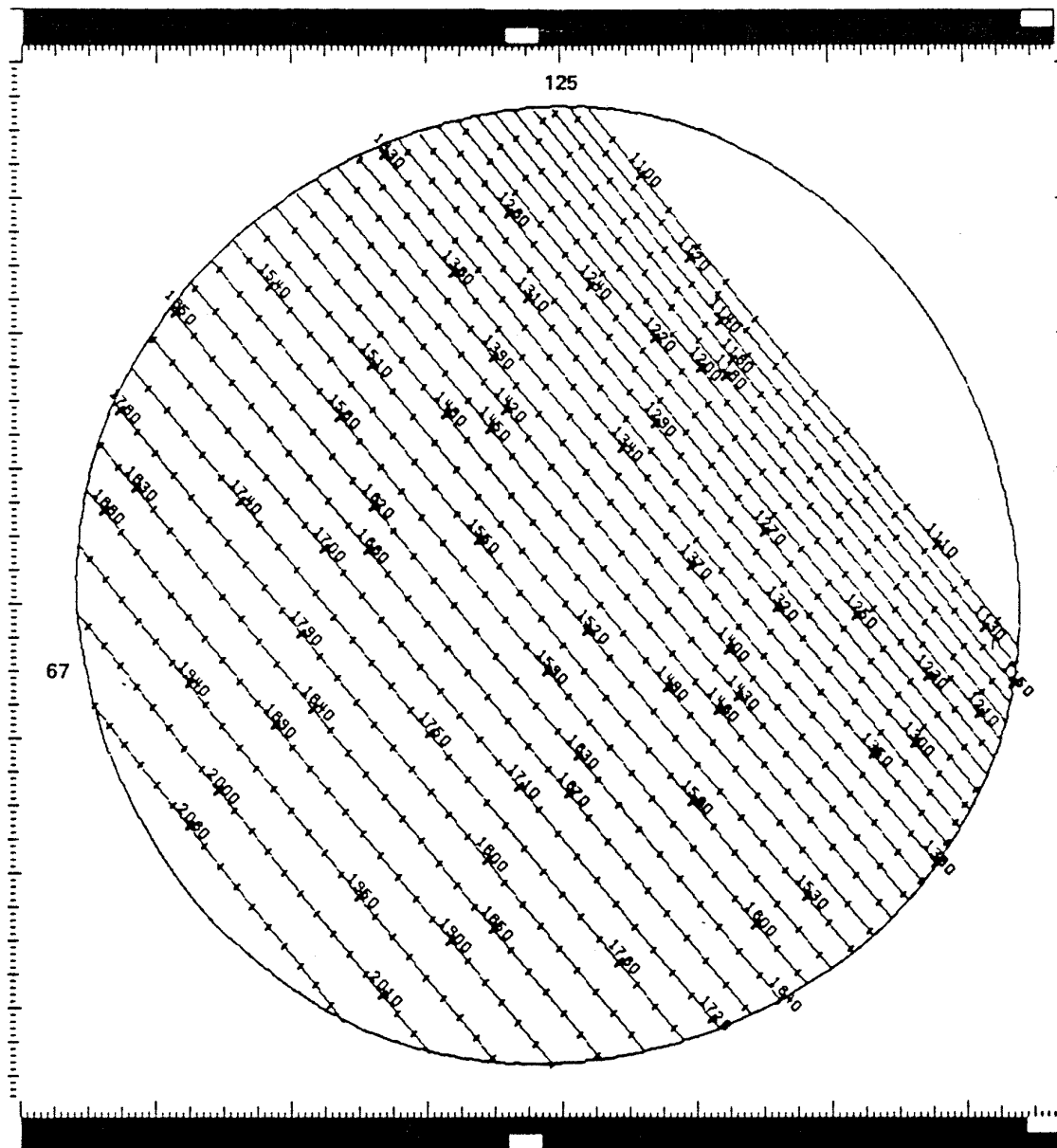


Figure 2.14: SWP large-aperture high-dispersion (odd orders) format.

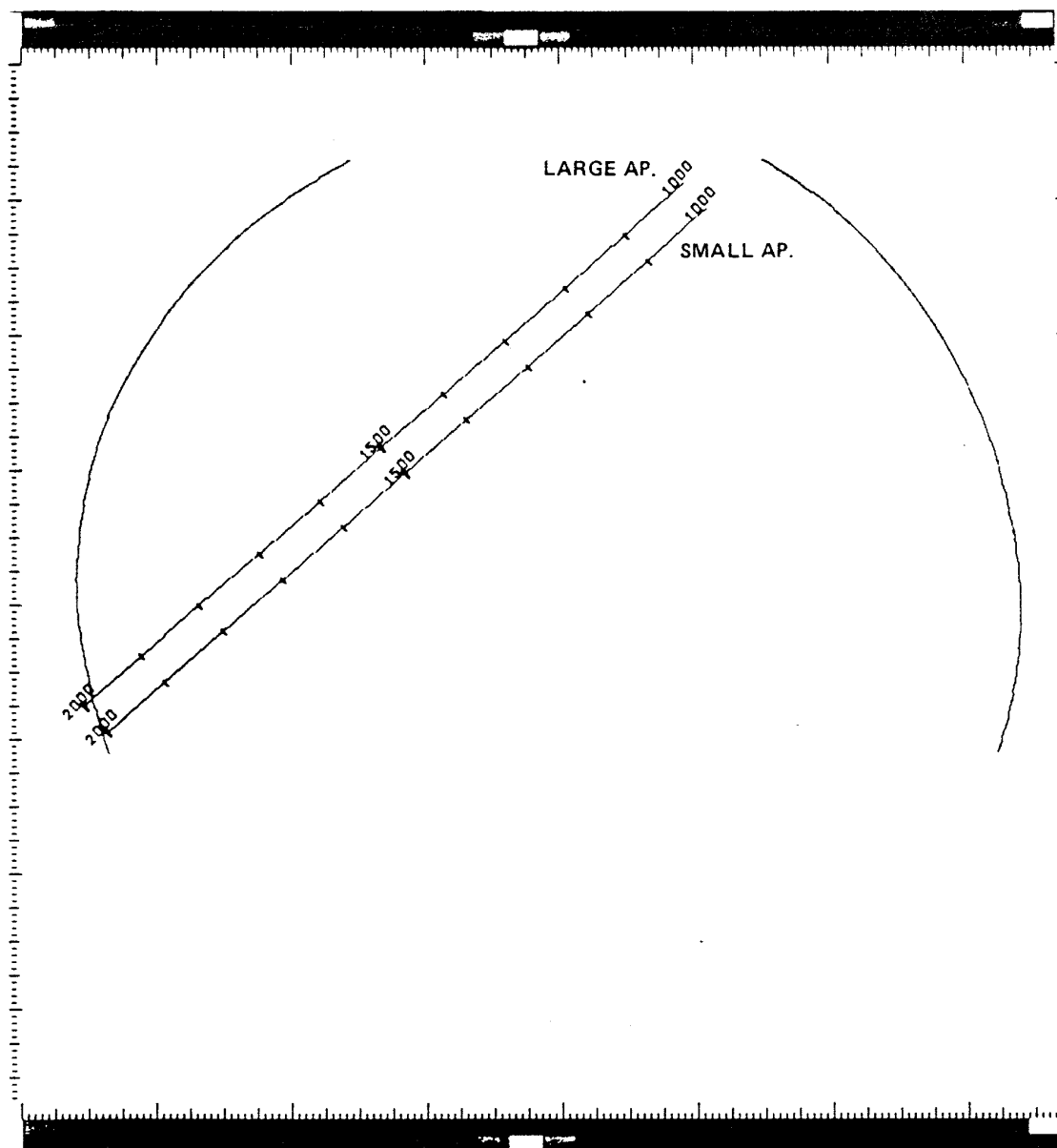


Figure 2.15: SWP large- and small-aperture low-dispersion format.

Table 2.2: Standard Offsets from the Small to the Large Spectrograph Aperture as used by low-dispersion NEWSIPS (in pixels)

| Camera | Along Dispersion | \perp to Dispersion | Total Offset |
|--------|------------------|-----------------------|--------------|
| LWP | -2.3 | 26.2 | 26.3 |
| LWR | -2.3 | 26.4 | 26.5 |
| SWP | 0.8 | 26.1 | 26.1 |

have been incorporated into the geometric correction step such that the wavelength scales for the small and large apertures are aligned.

The geometry of the two entrance apertures in relation to the image scan lines and the high and low resolution dispersion directions are shown in Figures 2.16 through 2.18 for the LWP, LWR, and SWP cameras. Note particularly the fact that the displacement between the short-wavelength large aperture (SWLA) and the short-wavelength small aperture (SWSA) is very nearly along the echelle dispersion direction. Therefore, short-wavelength high-dispersion images in which both apertures are exposed will result in nearly complete superposition of the large- and small-aperture spectra (with a wavelength offset). The displacement of the long-wavelength large aperture (LWLA) and the long-wavelength small aperture (LWSA) is less coincident with the echelle dispersion direction in this spectrograph, so that superposition of large- and small-aperture high-dispersion spectra is not as serious in the long-wavelength spectrograph.

For the purposes of judging the extent and separation of the apertures in the spectral domain, the scales given in Table 2.3 may be used in conjunction with the quantities in Tables 2.1 and 2.2. Note that in high dispersion a given shift along the dispersion corresponds closely to a constant Doppler velocity shift, whereas in low dispersion a given shift corresponds to a constant wavelength shift.

Table 2.3: Approximate Spectral Scales in Each Dispersion Mode

| Camera | Low ($\text{\AA}/\text{px}$) | High (km/s/px) |
|--------|--------------------------------|----------------|
| LWP | 2.66 | 7.21 |
| LWR | 2.66 | 7.27 |
| SWP | 1.68 | 7.72 |

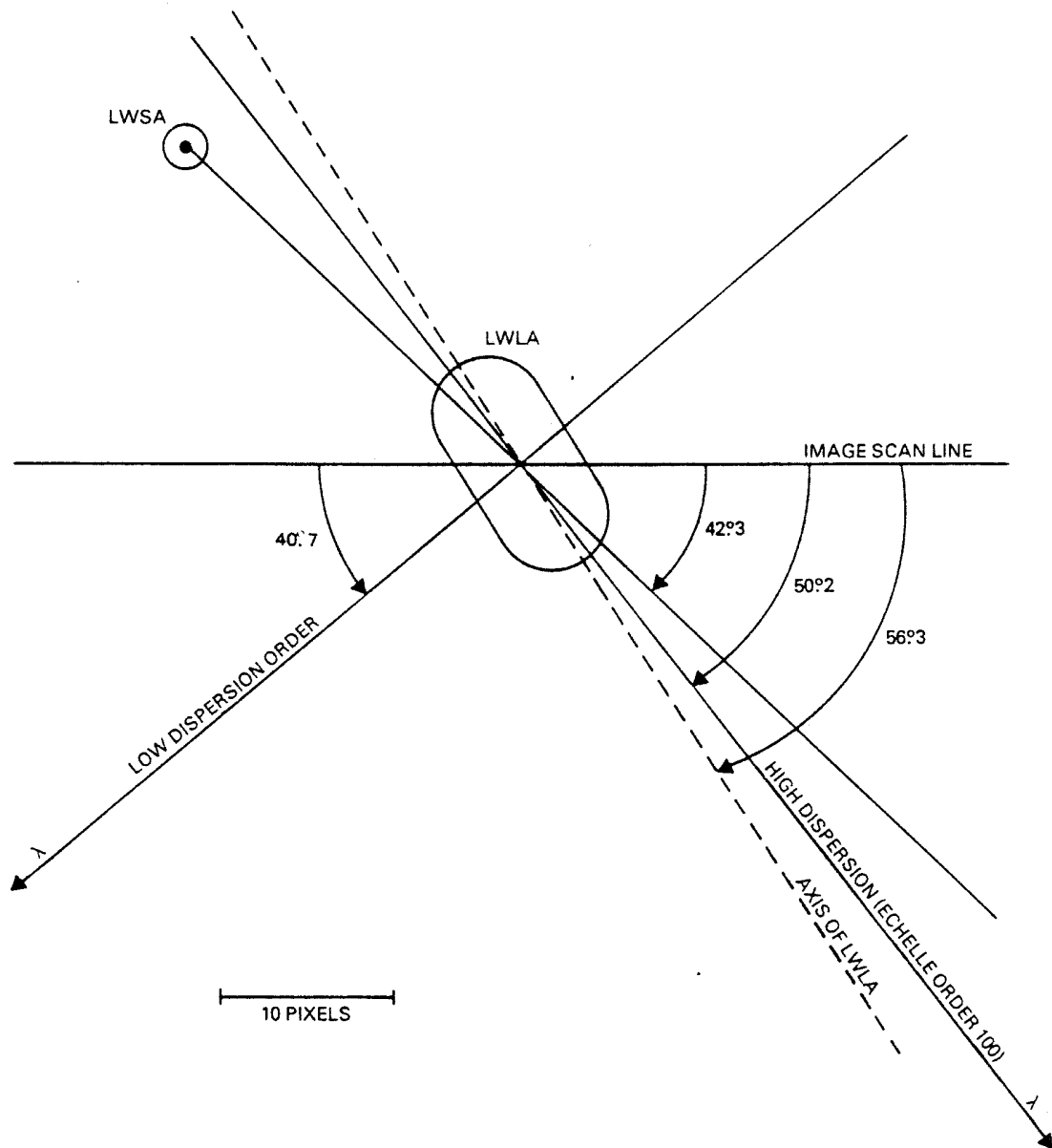


Figure 2.16: LWP Geometry

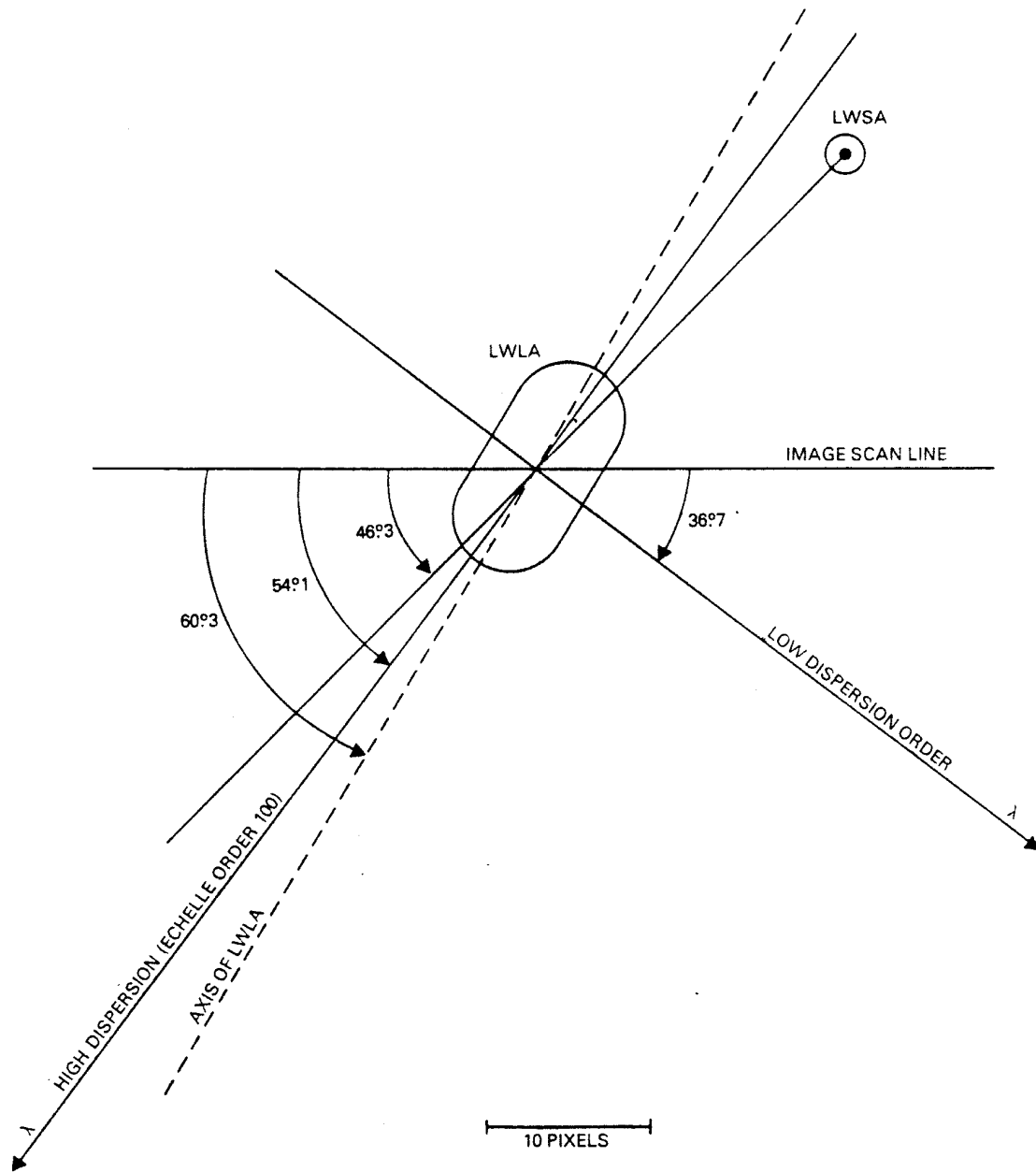


Figure 2.17: LWR Geometry

2.3 Instrumental Resolution

The instrumental resolution (both spectral and spatial) is a convolution of the camera resolution, dispersion mode, spectrograph entrance aperture, telescope focus, and spacecraft pointing stability. While the dominant effect is due to the camera, telescope focus and spacecraft pointing stability also play a major role in defining the resolution. In addition, it is well known that the camera resolution is highly wavelength dependent. According to the *IUE* Camera Users Guide (Coleman et al. 1977), the camera point spread function (PSF) consists of a narrow gaussian-like core having a full width at half maximum (FWHM) of 2 to 5 pixels and a weak long-range tail. The actual resolution in either the spatial or spectral direction can be defined as a function of the FWHM. The Rayleigh criterion of instrumental resolution specifies that two spectra (spatial direction) or two spectral features (spectral direction) can be resolved provided their separation is as follows (Weinstein and Pérez 1992):

$$d \geq 0.849 \times FWHM$$

where d is the distance separating the two features (or spectra). The gaussian fitting routine used in this analysis was GAUSSFITS, taken from the *IUE* Data Analysis Center software library. This procedure outputs the one-sigma width of the fitted gaussian profile which was then converted to FWHM using the statistical equality (Bevington 1969):

$$FWHM = 2.3548 \times \sigma$$

2.3.1 Low-Dispersion Mode

2.3.1.1 Resolution Along the Dispersion

A study of the NEWSIPS spectral resolution was performed by measuring the FWHM of several features for the emission line sources V1016 Cyg, RR Tel, AG Dra, CI Cyg, and Z And. The analysis indicates a slight improvement in the NEWSIPS resolution (approximately 10% for the SWP and 7% for the LWR) over the IUESIPS results reported by Cassatella, Barbero, and Benvenuti (1985). Plots of the spectral resolution data are shown in Figure 2.19. The small-aperture data are slightly offset in wavelength from the large-aperture data for clarity.

LWP – Large-aperture spectral resolution is best between 2700 and 2900Å with an average FWHM of 5.2Å and decreases to approximately 8.0Å on either side of this range. Small-aperture resolution is optimal between 2400 and 3000Å with an average FWHM of 5.5Å and decreases to 8.1Å at the extreme wavelengths.

LWR – Maximum resolution in the large aperture occurs longward of 2300Å, with an average FWHM of 5.3Å, while shortward of this point the FWHM decreases to 7.7Å. Small-aperture resolution is best from 2700–3200Å, with an average FWHM of 5.4Å, and decreases to 7.7Å at 3350Å and 7.5Å shortward of 2400Å.

SWP – The best resolution occurs around 1200Å, with a FWHM of 4.6Å in the large aperture and 3.0Å in the small aperture, and gradually worsens towards longer wavelengths: 6.7Å at 1900Å in the large aperture and 6.3Å in the small. On average, the small-aperture resolution is approximately 10% better than the large-aperture resolution.

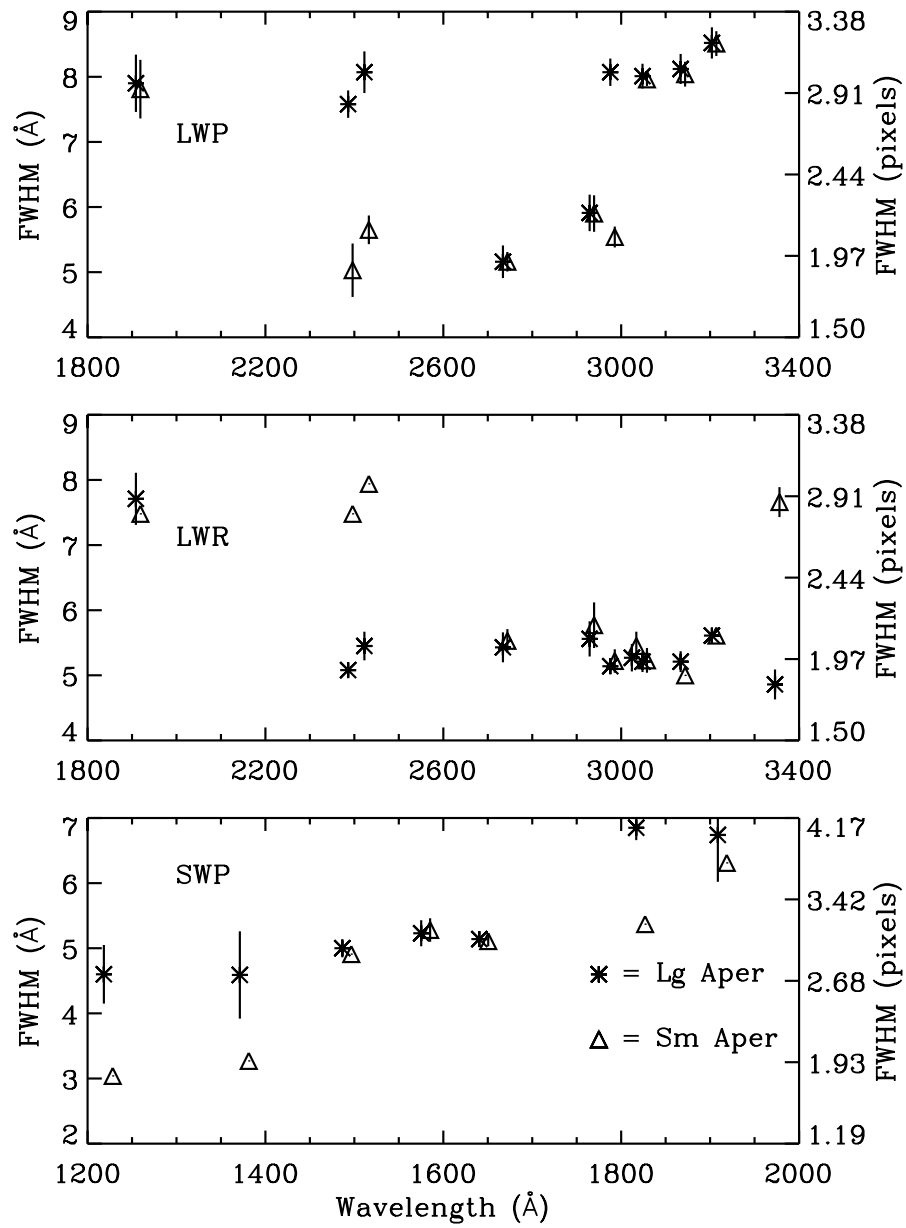


Figure 2.19: Low-dispersion spectral resolution.

2.3.1.2 Resolution Perpendicular to the Dispersion

The NEWSIPS spatial resolution has been determined by analyzing the spectra of several low-dispersion standard stars (*viz.*, HD 60753, HD 93521, BD+33° 2642, and BD+75° 325). The FWHM of large- and small-aperture spectra were measured at several wavelengths and plotted (see Figure 2.20). As is the case with the spectral resolution studies, the NEWSIPS values show, in general, an improvement over IUESIPS. As is the case with the spectral resolution plots, the small-aperture data are slightly offset from the large-aperture data.

LWP – The spatial resolution for the LWP is best near 3000Å where the FWHM for the large aperture is 2.4 pixels (3.6 arcsec), and decreases to values of around 3.0 pixels at the short- and long-wavelength ends of the spectrum. There is no significant difference between the large- and small-aperture spatial resolutions.

LWR – The behavior of the LWR camera as a function of wavelength is similar to the LWP, with the smallest FWHM values for the large aperture of 2.6 pixels (3.9 arcsec) occurring near 3000Å, and increasing to 3.6 and 3.0 pixels at the wavelength extremes. The small aperture, unlike the other two cameras, shows a dramatic *decrease* in resolution of approximately 10%.

SWP – The SWP camera shows the best spatial resolution near 1400Å with mean FWHM values for the large aperture of 2.7 pixels (4.1 arcsec), increasing slightly to 2.8 pixels at 1250Å, and 3.7 pixels at 1950Å. The SWP small-aperture resolution response is approximately the same as the large-aperture resolution.

2.3.2 High-Dispersion Mode

2.3.2.1 Resolution Along the Dispersion

A study of the spectral resolution in the high-dispersion mode was performed utilizing several methods. The first measured emission lines from small-aperture wavelength calibration (WAVECAL) images obtained using the on-board hollow cathode platinum-neon (Pt-Ne) calibration lamp. The second measured several features from the emission line sources V1016 Cyg and RR Tel and interstellar absorption line features from the calibration standard BD+75° 325. The third method measured absorption features from the calibration standard HD 149757 (Zeta Oph). The WAVECAL images are useful in determining the spectral resolution as they are not affected by the telescope focus nor are they subject to astrophysical broadening. The Zeta Oph spectra are characterized by very narrow interstellar absorption features so they are also useful for measuring spectral resolution. Therefore, the measurements taken from WAVECAL and Zeta Oph images represent the best possible spectral resolution obtainable.

LWP – The WAVECAL and large-aperture Zeta Oph resolution data are displayed in Figures 2.21 and 2.24, respectively. The results, along with the associated one-sigma error bars and linear fits (dashed line), are plotted as a function of order number in both wavelength and pixel space. The dotted line in the pixel space plots is the average of the resolution data over all orders. No small-aperture high-dispersion data of Zeta Oph is available. In addition,

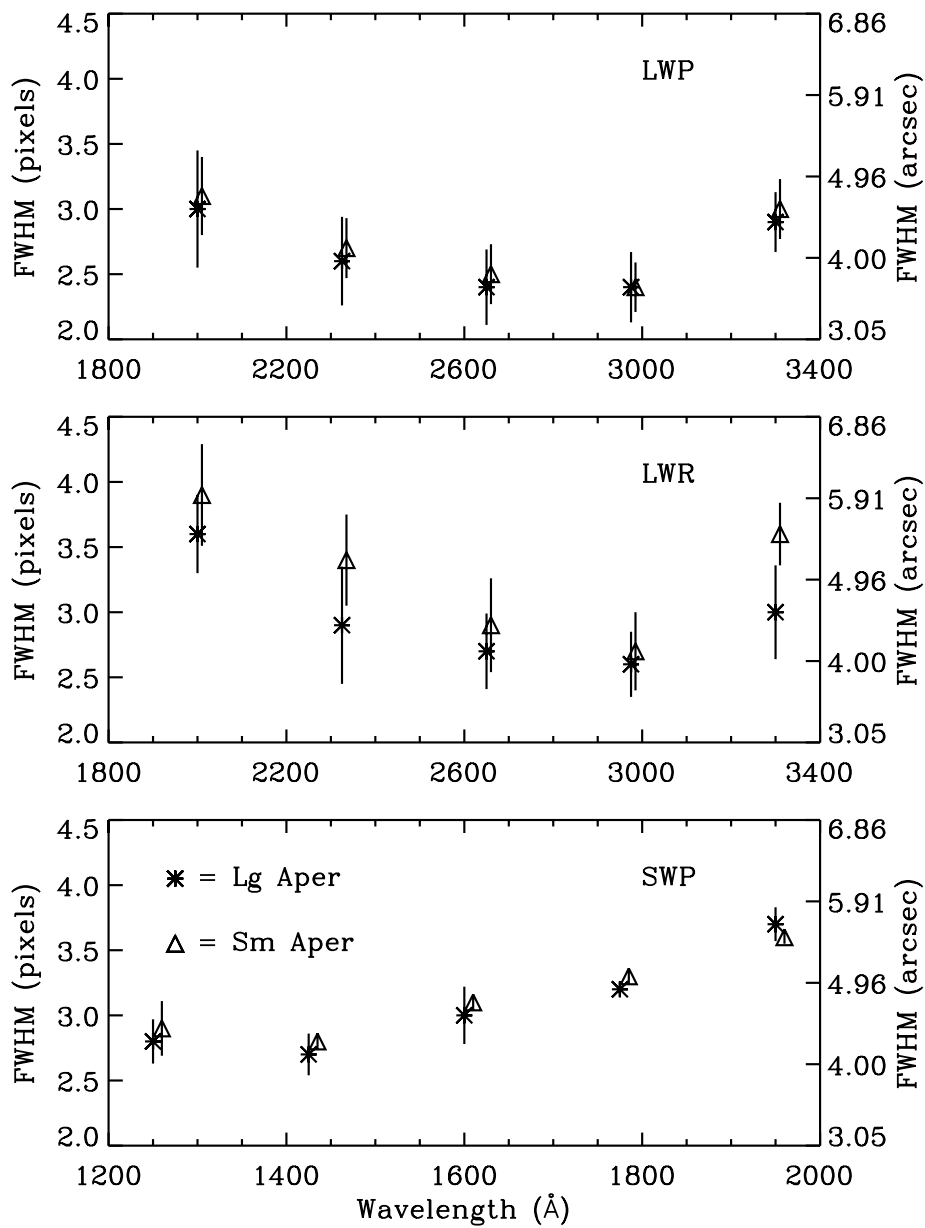


Figure 2.20: Low-dispersion spatial resolution.

the standard star, RR Tel, and V1016 Cyg data were too noisy to yield suitable results. The large-aperture Zeta Oph measurements are quite similar to the small-aperture WAVECAL analysis. The spectral resolution in wavelength space is approximately 0.18\AA FWHM at order 75 and linearly decreases (roughly) to 0.11\AA at order 117. The pixel space data for both WAVECALs and Zeta Oph show the same improvement in resolution between orders 95 and 110.

The *IUE* Systems Design Report (GSFC 1976) lists $15,000 (\lambda/\Delta\lambda)$ as the high-dispersion resolution for the long-wavelength cameras. This yields 0.22\AA for order 69, 0.17\AA for order 90, and 0.13\AA for order 123. These numbers are comparable to the NEWSIPS results of 0.24\AA , 0.15\AA , and 0.12\AA for these same orders. An analysis of IUESIPS spectral resolution was performed by Evans and Imhoff (1985) using FWHM measurements obtained from WAVECAL images. The results are as follows: 0.22\AA for order 75, 0.17\AA for order 83, 0.13\AA for order 96, and 0.13\AA for order 116. These figures are very similar to the NEWSIPS results of 0.20\AA , 0.14\AA , 0.15\AA , and 0.13\AA .

LWR – The WAVECAL spectral resolution measurements are shown in Figure 2.22 along with the corresponding linear fit (dashed line) and average (dotted line). The FWHM trends (wavelength space) below order 80 are quite similar to the LWP figures (i.e., a linear dependence of FWHM on order number). The camera resolution in wavelength space is nearly constant for orders 80 through 115, with a slight degradation in LWR resolution above order 115. This trend is easily visible in the the pixel space resolution plot and is evident from the deviation of the FWHM measurements from the mean (dotted line).

Cassatella et al. (1981) and Cassatella and Martin (1982) report a nearly constant FWHM (wavelength space) as a function of order number for WAVECAL images processed through IUESIPS. The average FWHM from their analysis is approximately 0.18\AA above order 81; a value which is higher than the corresponding NEWSIPS FWHM of 0.14\AA . They report a FWHM of 0.22\AA for order 72, which again is much higher than the NEWSIPS results of 0.19\AA . Evans and Imhoff (1985) also measured spectral resolution using IUESIPS processed WAVECAL images. They present FWHM values of 0.19\AA , 0.17\AA , 0.16\AA , and 0.15\AA for orders 75, 83, 96, and 116, respectively. The corresponding NEWSIPS values for these same orders are: 0.19\AA , 0.14\AA , 0.15\AA , and 0.14\AA . Boggess et al. (1978) quote a constant FWHM of 0.19\AA for WAVECAL images, regardless of order number. This contradicts all subsequent reports written on this subject as well as the NEWSIPS results shown here. Their analysis was performed early in the life of *IUE*; perhaps the camera characteristics had not yet stabilized at this period in time.

SWP – The WAVECAL, Zeta Oph, and large- and small-aperture stellar source spectral resolution data are displayed in Figures 2.23, 2.25, 2.26, and 2.27. As is the case with the LWP and LWR, the plots include one-sigma error bars and linear (dashed line) and mean (dotted line) fits to the data. In Figures 2.26 and 2.27, the emission line measurements for orders 111 and above were excluded from the analysis when performing the linear fit to the stellar data because they were highly discrepant. The spectral resolution in wavelength space for the WAVECAL, Zeta Oph, and stellar source images shows no dependence on wavelength within an order and a roughly linear dependence on order number. Unlike the

LWP, the SWP resolution from the Zeta Oph analysis (Figure 2.25) is much worse than the corresponding WAVECAL data (Figure 2.23). The stellar source results are somewhat inconclusive for orders 111 and above. The emission line widths are dramatically higher than the corresponding absorption line measurements. This trend was also seen in the analysis by Grady (1985). The *IUE* Systems Design Report (GSFC 1976) quotes a figure of 10,000 ($\lambda/\Delta\lambda$) for the spectral resolution in high-dispersion mode. This corresponds to a FWHM of approximately 0.2\AA for order 66 and 0.1\AA for order 125. This same trend is seen in the top plot (Figure 2.23) of the WAVECAL resolution analysis; the spectral resolution is essentially a constant value in pixel space (bottom plot). The stellar source resolution measurements in pixel space (bottom plot of Figures 2.26 and 2.27) show some degradation towards higher order numbers. In addition, the small-aperture data (Figure 2.27) indicates an 8% improvement in resolution over the large-aperture counterpart (Figure 2.26).

The general trend of the wavelength-space resolution for the WAVECAL images is approximately the same for every IUESIPS study that has been reviewed (i.e., Boggess et al. 1978, Cassatella et al. 1981, Cassatella and Martin 1982, and Evans and Imhoff 1985). That is, the camera resolution in wavelength space varies roughly linearly with order number and improves towards shorter wavelengths (0.19\AA for order 69 and 0.09\AA for order 106). The results from analysis of WAVECAL images processed through NEWSIPS are almost identical to these figures. Penston (1979) reported SWP large-aperture FWHM values of 0.20\AA for absorption lines and 0.24\AA for emission lines. These figures are comparable with the average NEWSIPS results of 0.21\AA and 0.23\AA respectively. However, Penston's (1979) measurements for the small-aperture resolution are no better than the large aperture. This result could be supported by the NEWSIPS analysis as the apparent improvement in small-aperture resolution is less than the one-sigma error of the FWHM average for any given order. Grady (1985) assessed the effects of the two-gyro control mode on high-dispersion data using large-aperture RR Tel spectra. The mean resolution (averaged over all orders) from the Grady analysis (0.22\AA) agrees with the average NEWSIPS resolution result.

2.3.2.2 Resolution Perpendicular to the Dispersion

The spatial resolution has been determined by analyzing the spectra of high-dispersion standard stars. The FWHM of several pairs of large and small-aperture line-by-line images were measured at five sample positions (*viz.*, 134, 258, 384, 507, and 615). For each sample position, a three pixel wide average cross-cut perpendicular to the dispersion was taken and the widths of the orders measured using the gaussian fitting routine. The results for each image were in good agreement, so we averaged the results to yield a set of spectral widths for each aperture as a function of order number and sample position. The differences in telescope focus between the images were kept small so as to minimize the effect of focus on the resolution measurements (Pérez et al. 1990). The database of spectra used for each camera contains a combination of optimally exposed images for the central orders and overexposed (in the central orders only) images for the extreme orders. The spatial resolution data and the one-sigma error bars for each sample position are plotted as a function of order number.

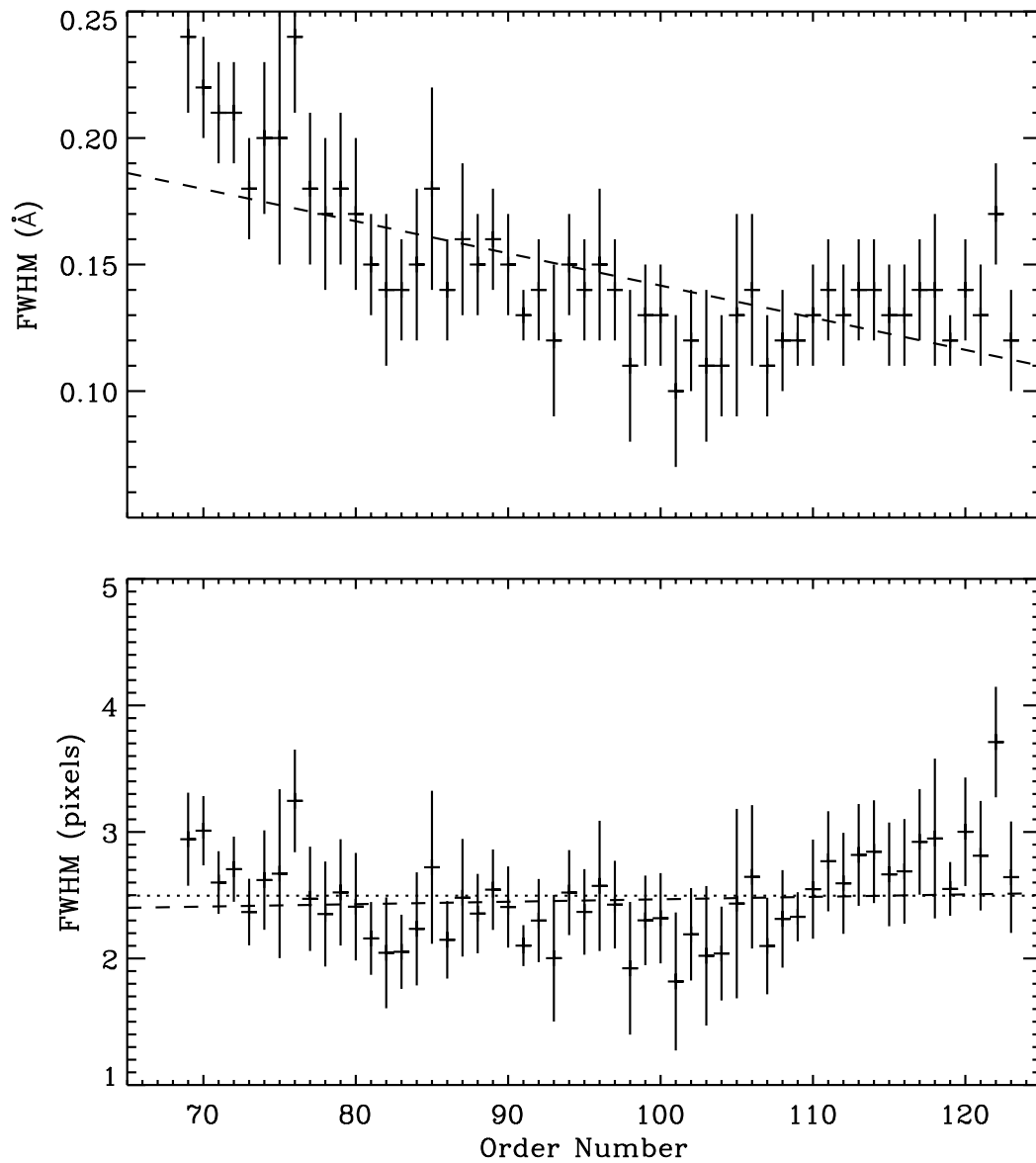


Figure 2.21: LWP high-dispersion spectral resolution from WAVECAL analysis.

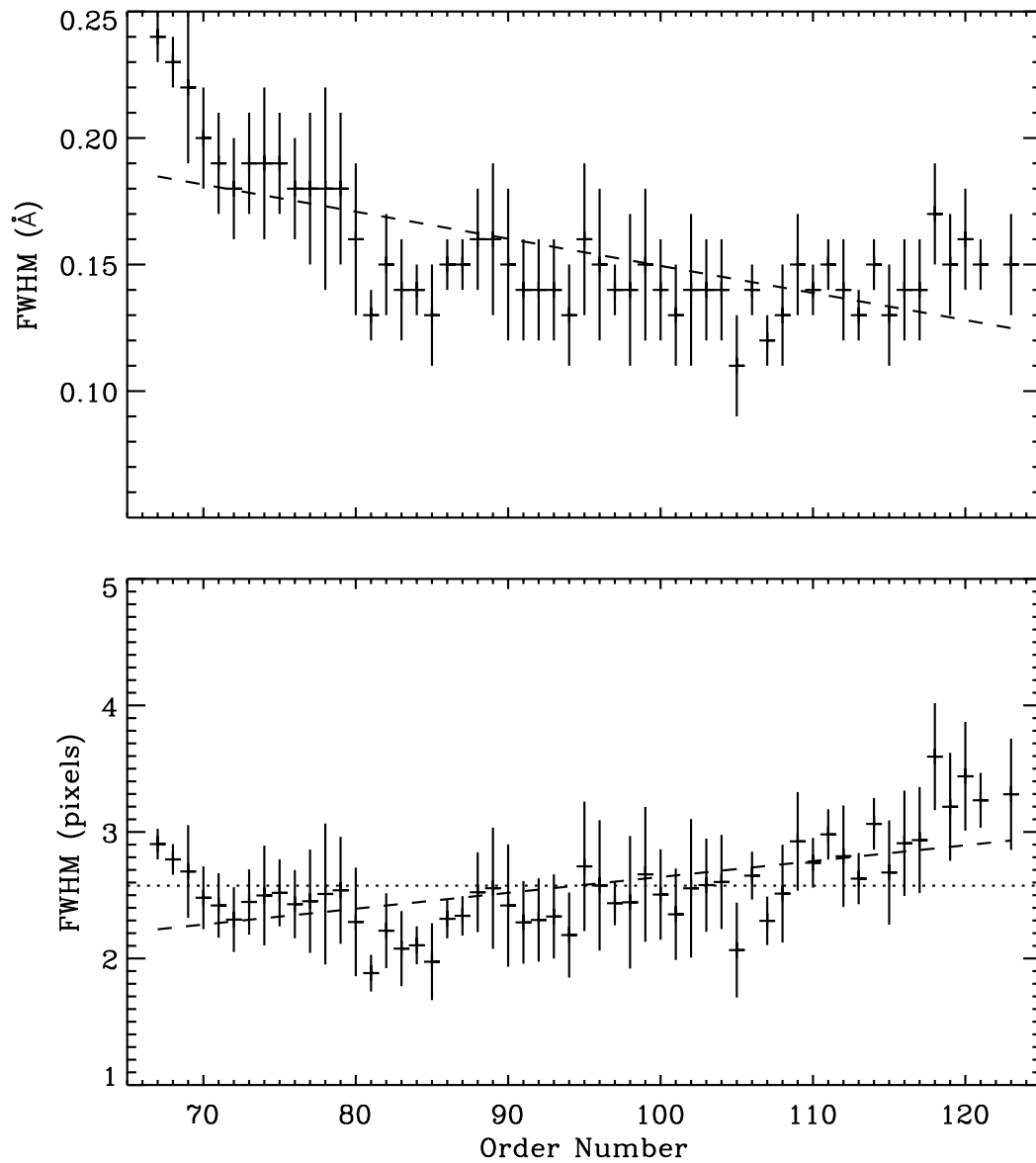


Figure 2.22: LWR high-dispersion spectral resolution from WAVECAL analysis.

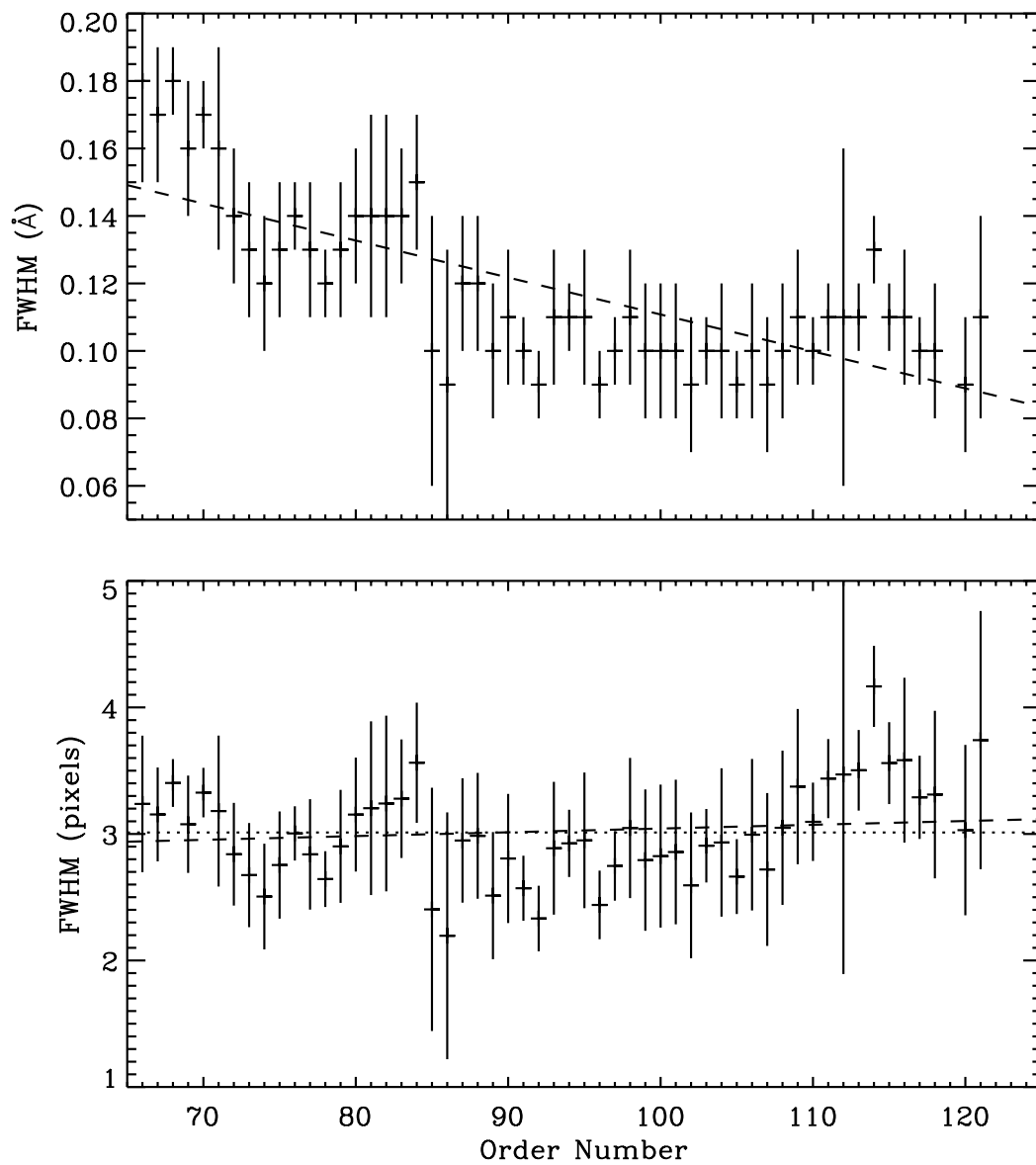


Figure 2.23: SWP high-dispersion spectral resolution from WAVECAL analysis.

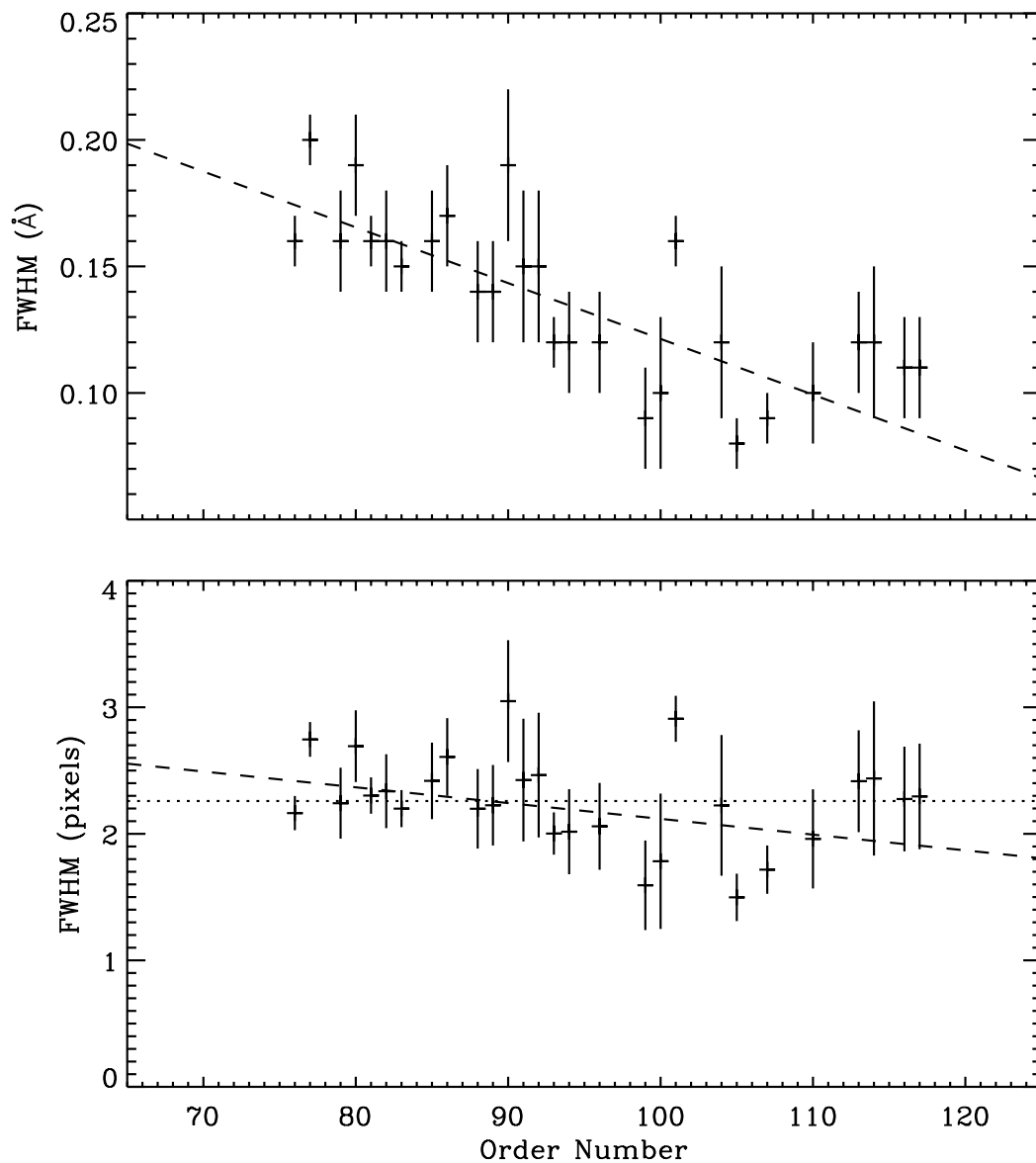


Figure 2.24: LWP high-dispersion spectral resolution from analysis of large-aperture Zeta Oph data.

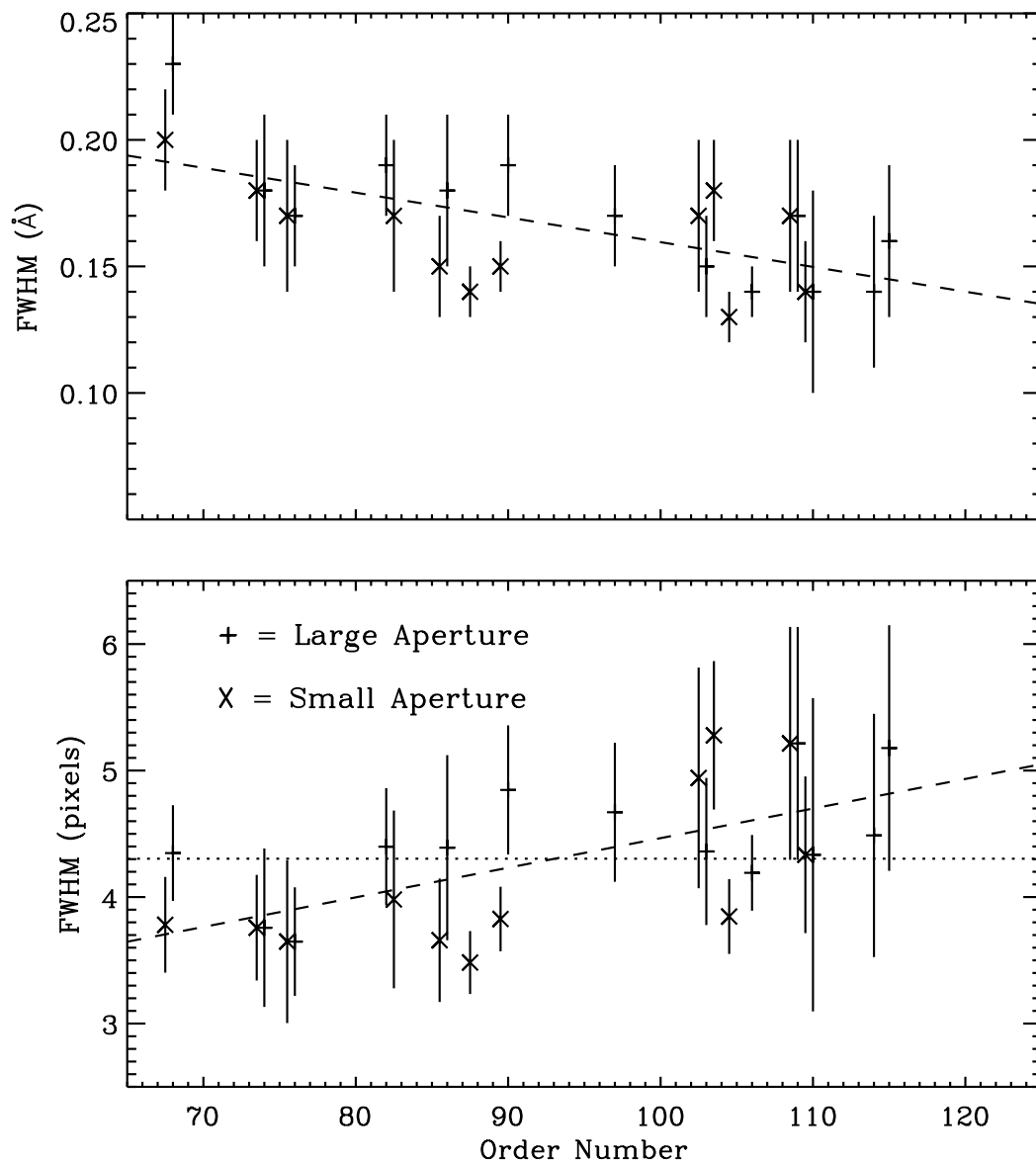


Figure 2.25: SWP high-dispersion spectral resolution from analysis of large- and small-aperture Zeta Oph data. Small-aperture data is horizontally offset to the left of the large-aperture data by half an order.

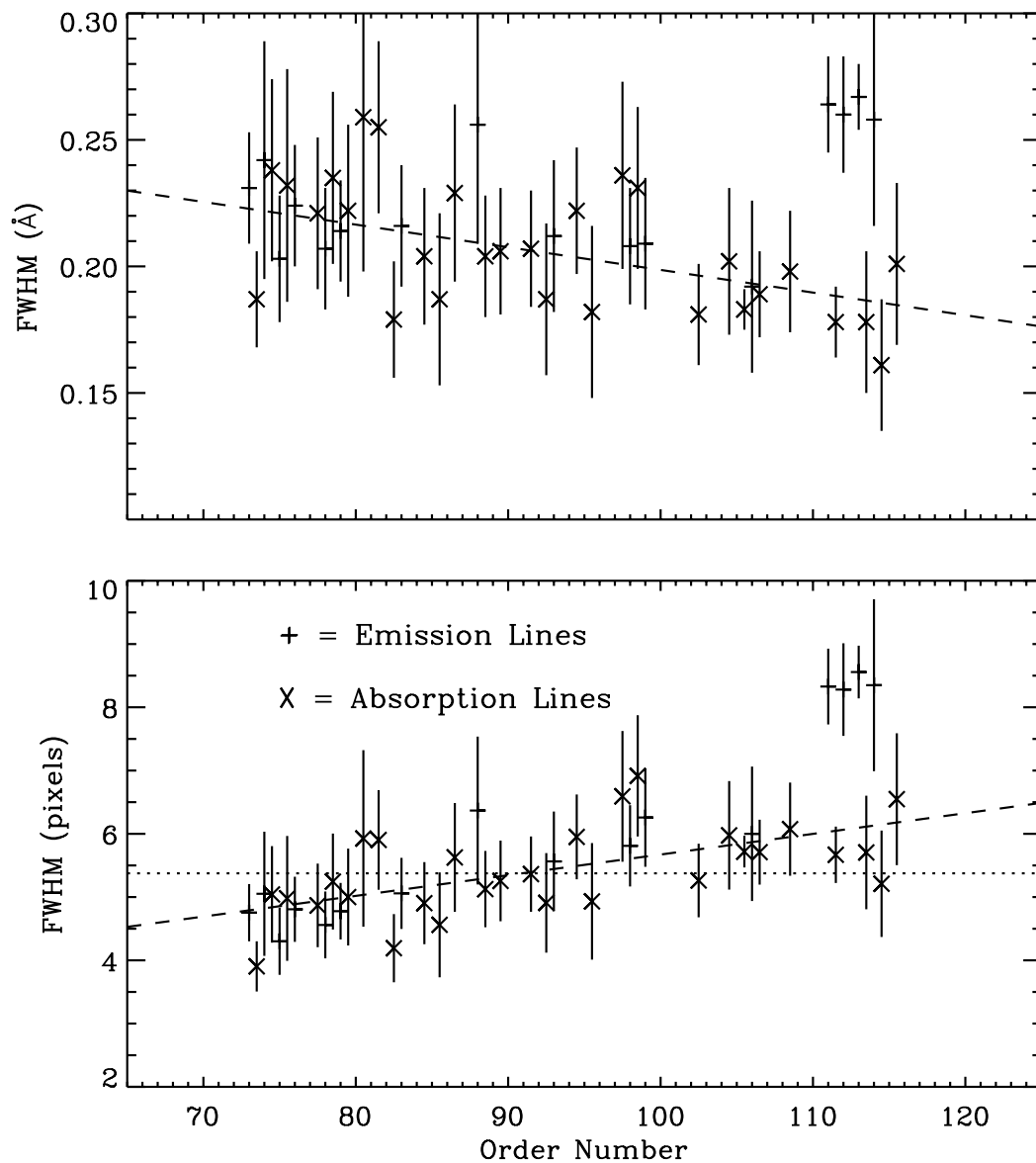


Figure 2.26: SWP high-dispersion spectral resolution from large-aperture stellar source analysis. Absorption line data is horizontally offset to the left of the emission line data by half an order.

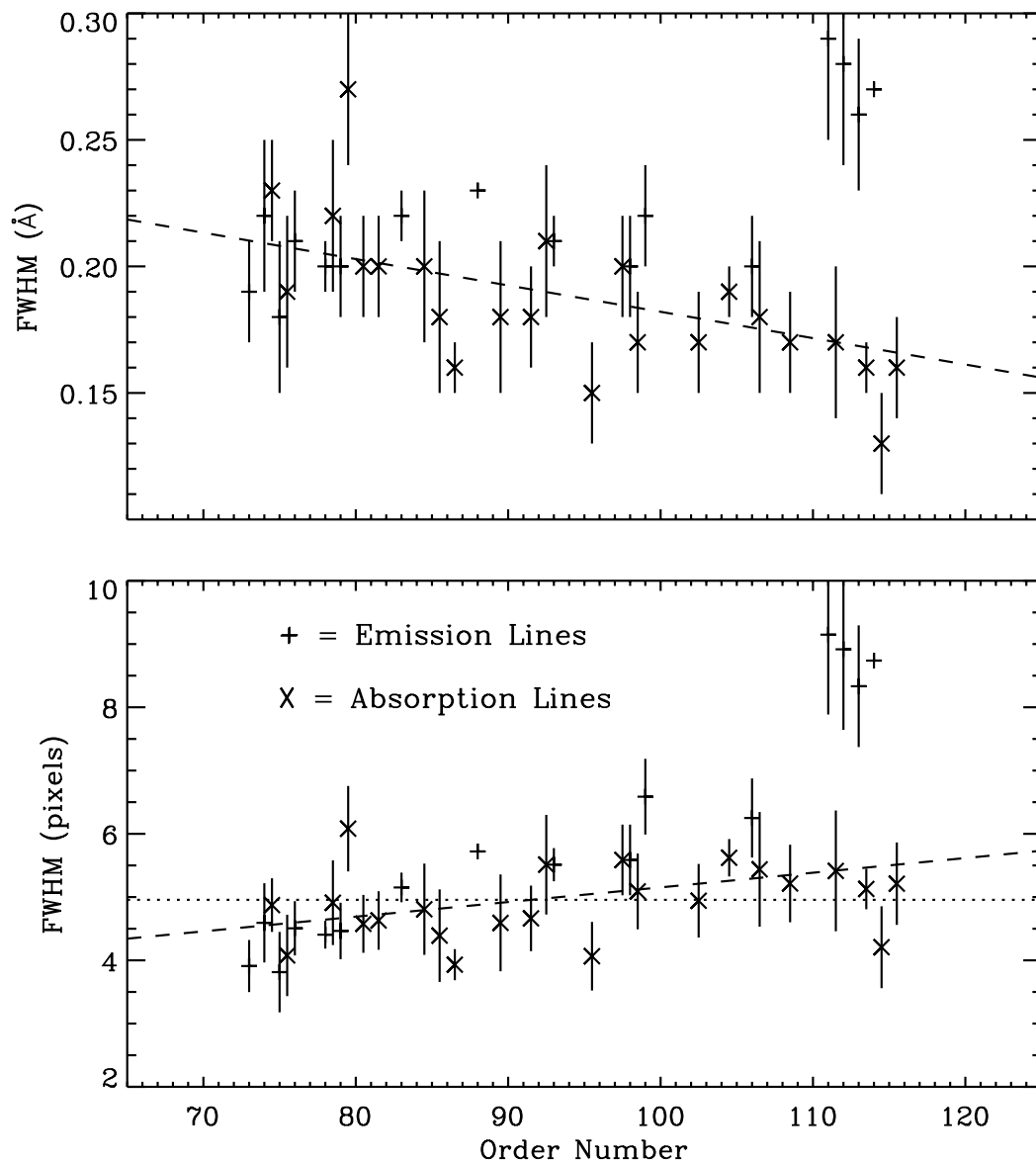


Figure 2.27: SWP high-dispersion spectral resolution from small-aperture stellar source analysis. Absorption line data is horizontally offset to the left of the emission line data by half an order.

The small-aperture data are horizontally offset to the left of the large-aperture data by half an order for clarity. A seventh-order polynomial fit to the data is also provided.

LWP – Spatial resolution measurements of the FWHM are plotted in Figures 2.28–2.32. The spatial resolution for sample position 384 is approximately 3.5 pixels FWHM at order 69 and decreases to 2.3 pixels at order 80 where it is roughly constant for the remaining orders. The spatial resolution degrades as one moves towards smaller sample positions and improves slightly (as compared with sample position 384) above order 90 for sample position 507. Small-aperture resolution shows an average improvement (over all orders and sample positions) of 4.6% over the large aperture. This difference is most apparent between orders 80 through 100 and at the smaller sample positions where it is as much as 8% for sample position 134. Unfortunately, no LWP high-dispersion spatial resolution studies could be found for IUESIPS data to compare against the NEWSIPS results.

LWR – Figures 2.33–2.37 show spatial resolution measurements of the FWHM plotted as a function of order number. The resolution trends for sample positions 134 through 384 are quite similar. The FWHM is approximately 3.0 pixels for order 69 and linearly decreases to 2.4 pixels at order 80 where it remains fairly constant for the remaining orders. For sample position 507, the FWHM is around 3.2 pixels for order 69 and linearly decreases to 2.6 pixels at order 80 where it then gradually decreases to 2.3 pixels at order 123. The behavior for sample position 615 demonstrates a rapid decrease in FWHM from 3.8 pixels at order 69 to 2.7 pixels at order 95 where it then gradually decreases to 2.3 pixels at order 120. The small-aperture resolution shows an improvement of approximately 4.7% over the large aperture.

The IUESIPS FWHM measurements obtained by Cassatella et al. (1981) using WAVE-CAL images are somewhat inconclusive. Their data only includes 5 orders (71, 73, 77, 81, and 90) and no mention was made of the sample positions at which these measurements were taken. Their numbers range from 3.5 pixels at order 71 to 2.7 pixels at order 90; values which are around 10% higher than the corresponding NEWSIPS FWHM measurements. The trends seen in the 2-D contour plots made by de Boer et al. (1983) are in good agreement with the NEWSIPS results. They show that for the central sample positions (i.e., 384) the FWHM starts out at 3.1 pixels at low order numbers and decreases to 2.8 pixels towards the center of the camera (e.g., order 90). The slight degradation in resolution seen in the central orders of Figure 2.35 is also apparent in the de Boer plots.

SWP – Spatial resolution measurements of the FWHM are plotted in Figures 2.38–2.42. The resolution trends as a function of order number are, in general, the same for every sample position. The FWHM is around 4 pixels at order 66 (long wavelengths) and decreases to approximately 2 pixels near order 100 (short wavelengths). Unlike the indications from previous IUESIPS studies (e.g., Bianchi (1980), Schiffer (1980), and Cassatella et al. (1981)), this decrease is not linear with order number. A plateau of around 3.0 pixels FWHM occurs between orders 75 and 85. This trend is confirmed by the analysis of de Boer et al. (1983), which displayed the order widths using 2-D contour plots. The FWHM remains fairly constant above order 100 for sample positions 258 and 384. At these sample positions, the higher orders (100 and above) are well away from the edge of the camera. The more

extreme sample positions (i.e., 134 and 507) show an edge effect as the resolution dramatically worsens above order 100. The best spatial resolution occurs near sample position 384 and worsens slightly as one moves towards smaller sample positions (i.e., shorter wavelengths within an order). Differences in resolution between the large and small apertures are small. The small aperture shows an average improvement (over all orders) of 2.4% in resolution over the large aperture.

As is the case with the low-dispersion resolution studies, the NEWSIPS values show an improvement over IUESIPS measurements. Schiffer (1980) quoted FWHM values of 3.5 pixels for order 75 and 2.4 pixels for order 105. The NEWSIPS results for those orders are 3.3 pixels and 2.1 pixels, respectively. Analysis by de Boer et al. (1983) showed the best resolution of 2.4 pixels FWHM occurring near the center of the camera. The NEWSIPS results indicate a FWHM of 2.0 pixels in this same area (sample position 384). Also, Bianchi (1980) expressed FWHM as a function of order number, regardless of camera, according to the following formula: $FWHM = 7.23 - 0.04 \times m$ where m is order number and the FWHM is in pixels. Thus, for order 71, this indicates a FWHM of 4.4 pixels, a figure that is almost 20% higher than the NEWSIPS average measurement for that order.

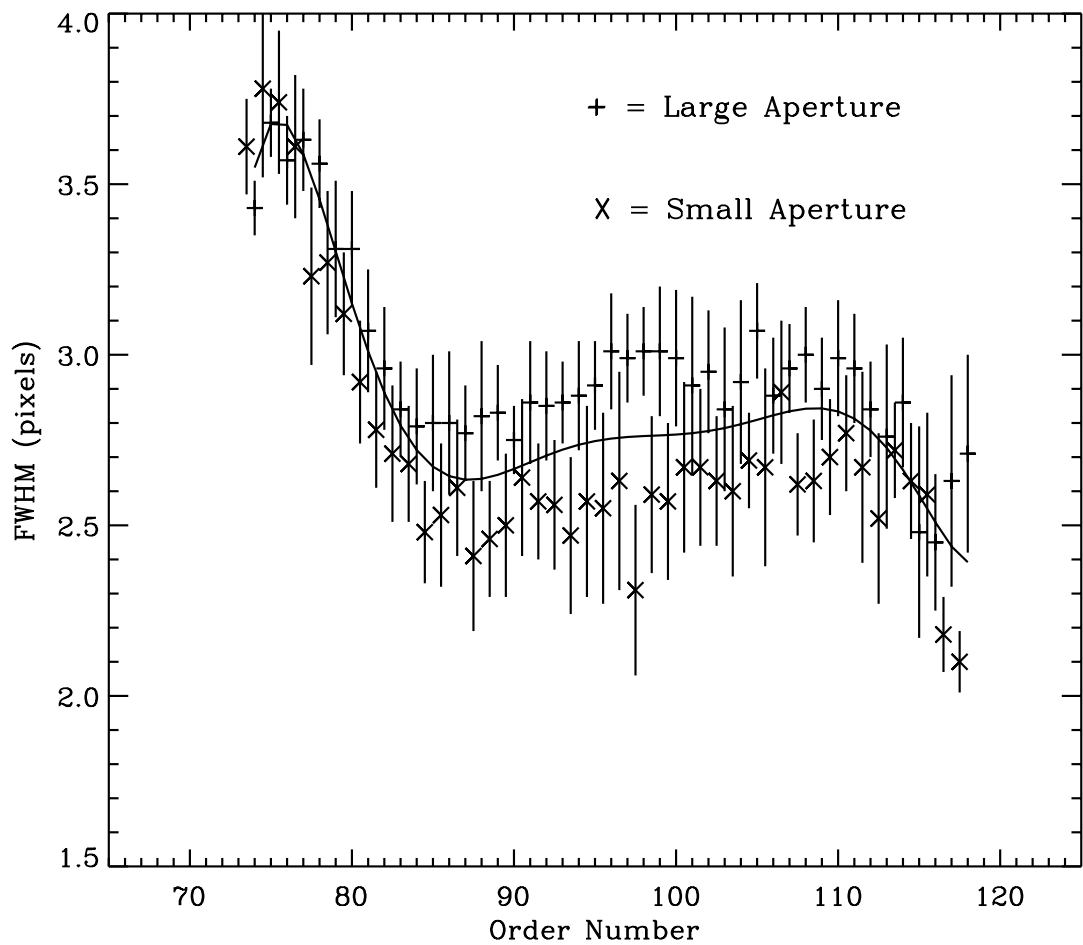


Figure 2.28: LWP high-dispersion spatial resolution for sample position 134. Small-aperture data is horizontally offset to the left of the large-aperture data by half an order.

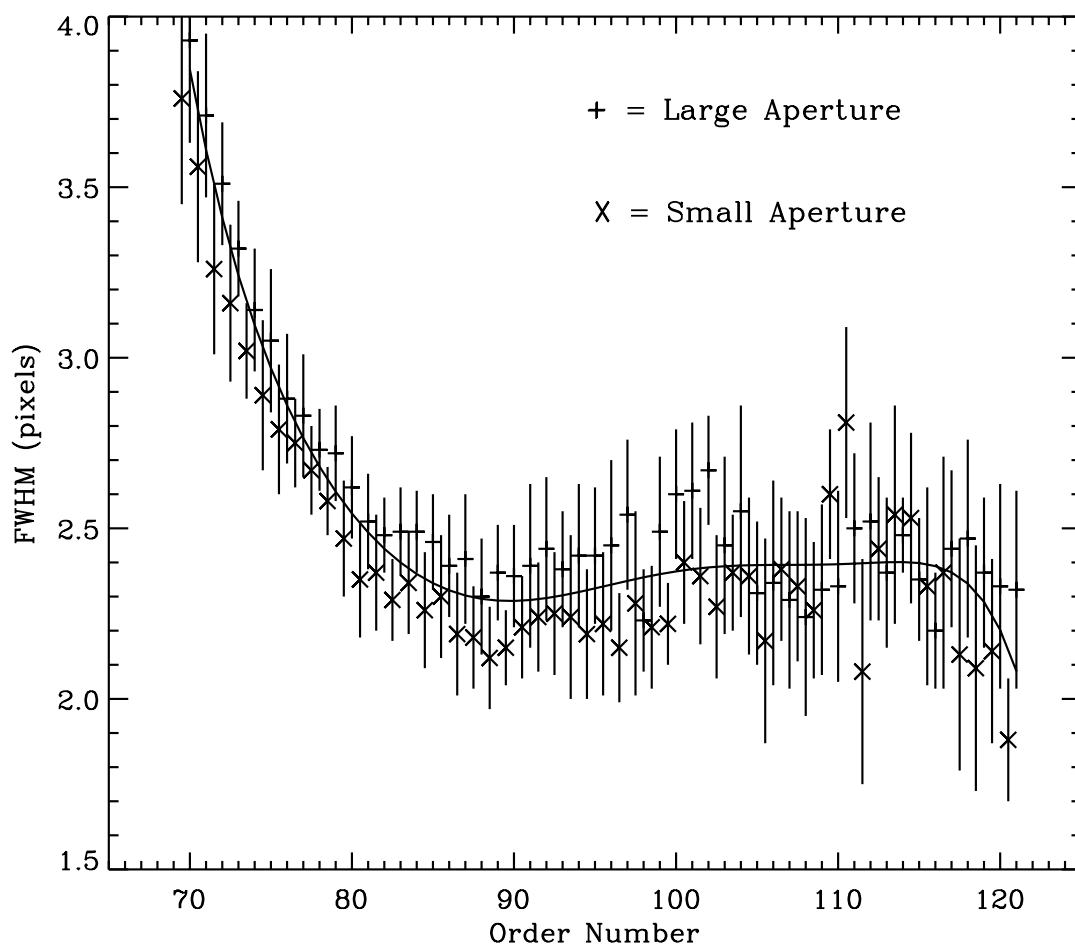


Figure 2.29: LWP high-dispersion spatial resolution for sample position 258. Small-aperture data is horizontally offset to the left of the large-aperture data by half an order.

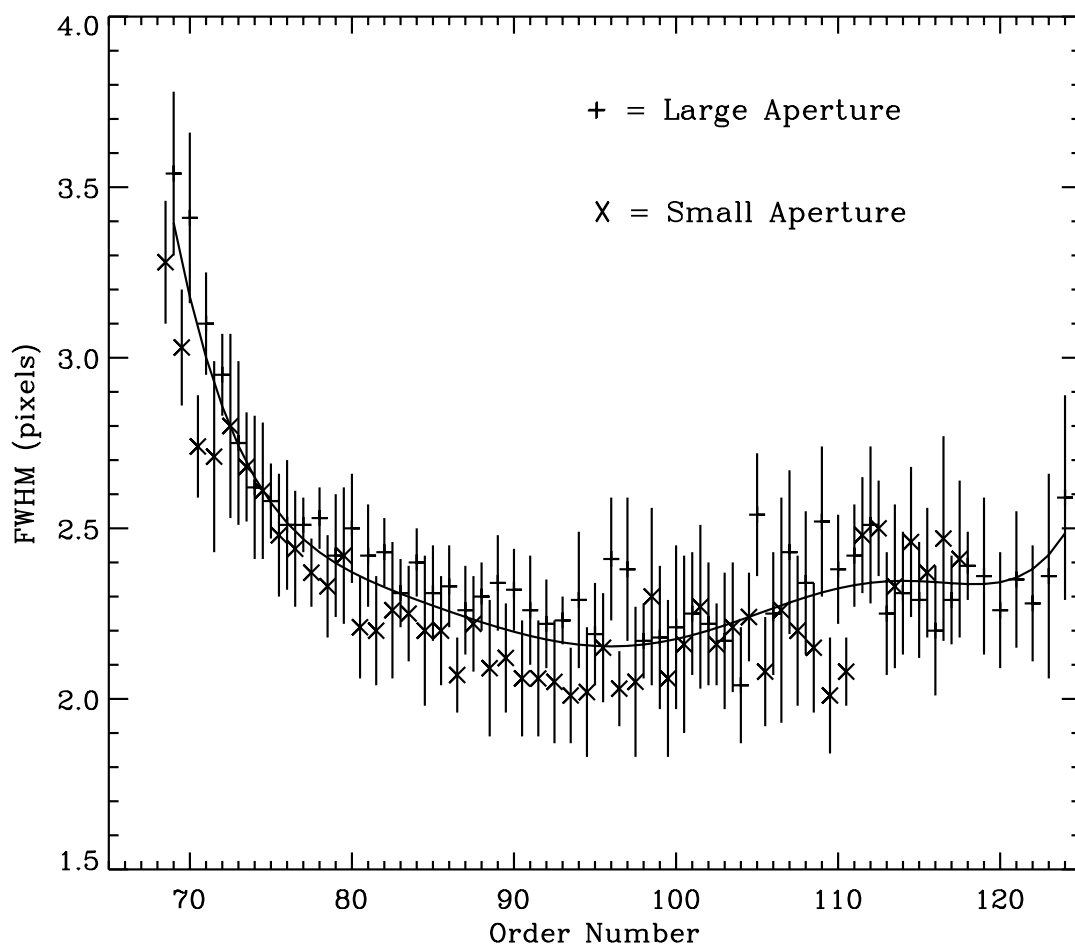


Figure 2.30: LWP high-dispersion spatial resolution for sample position 384. Small-aperture data is horizontally offset to the left of the large-aperture data by half an order.

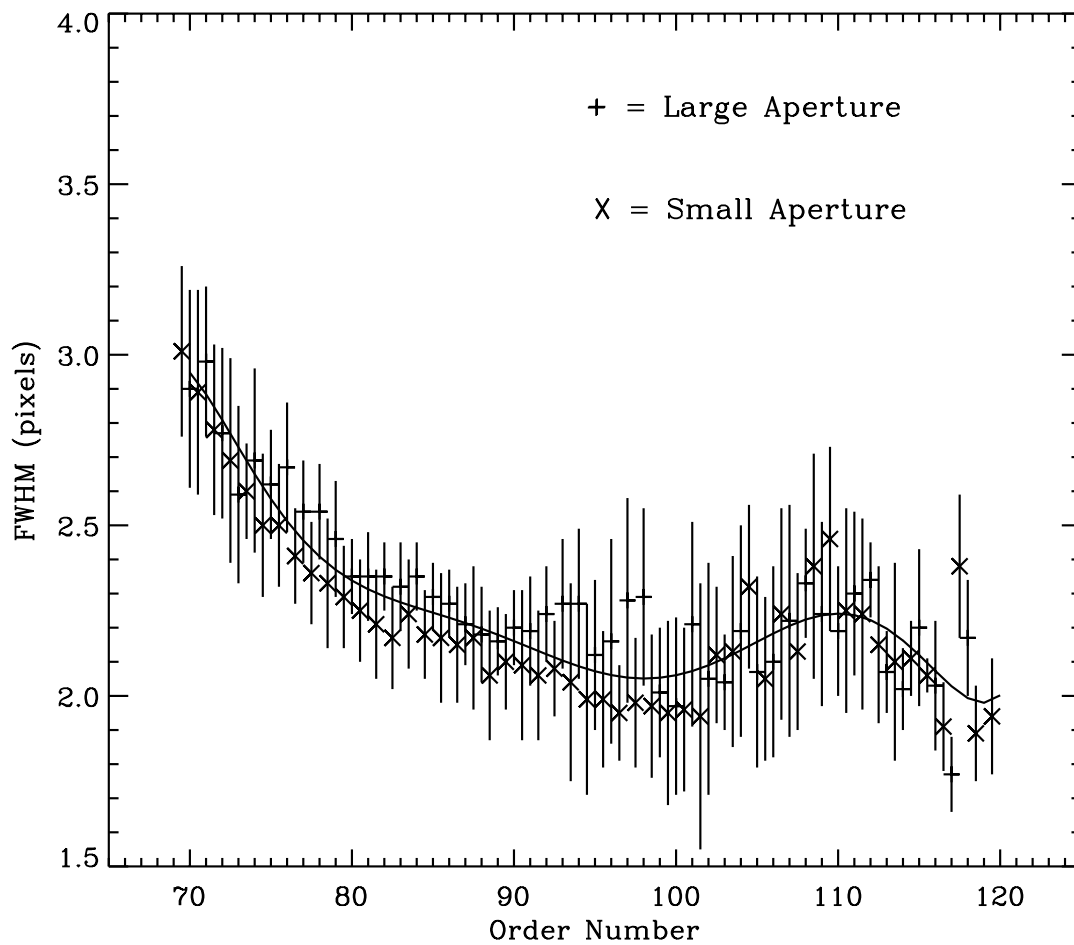


Figure 2.31: LWP high-dispersion spatial resolution for sample position 507. Small-aperture data is horizontally offset to the left of the large-aperture data by half an order.

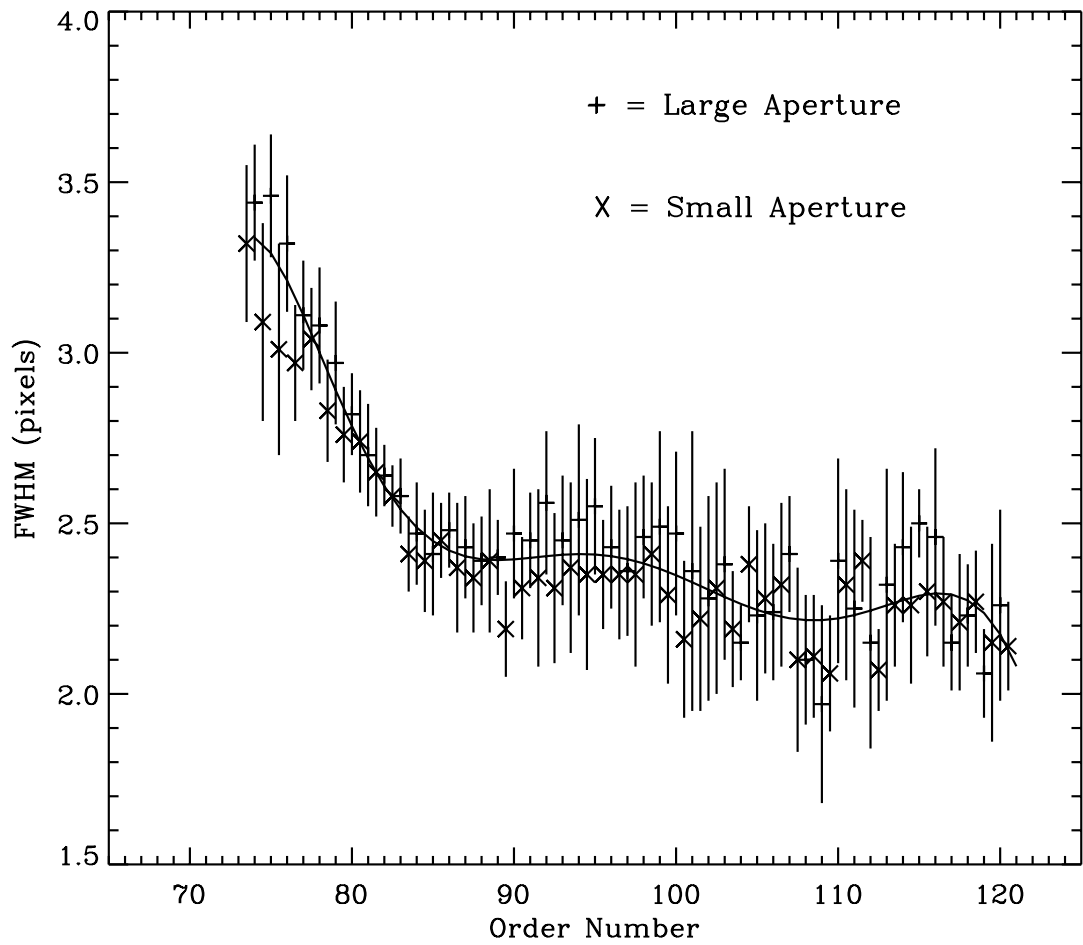


Figure 2.32: LWP high-dispersion spatial resolution for sample position 615. Small-aperture data is horizontally offset to the left of the large-aperture data by half an order.

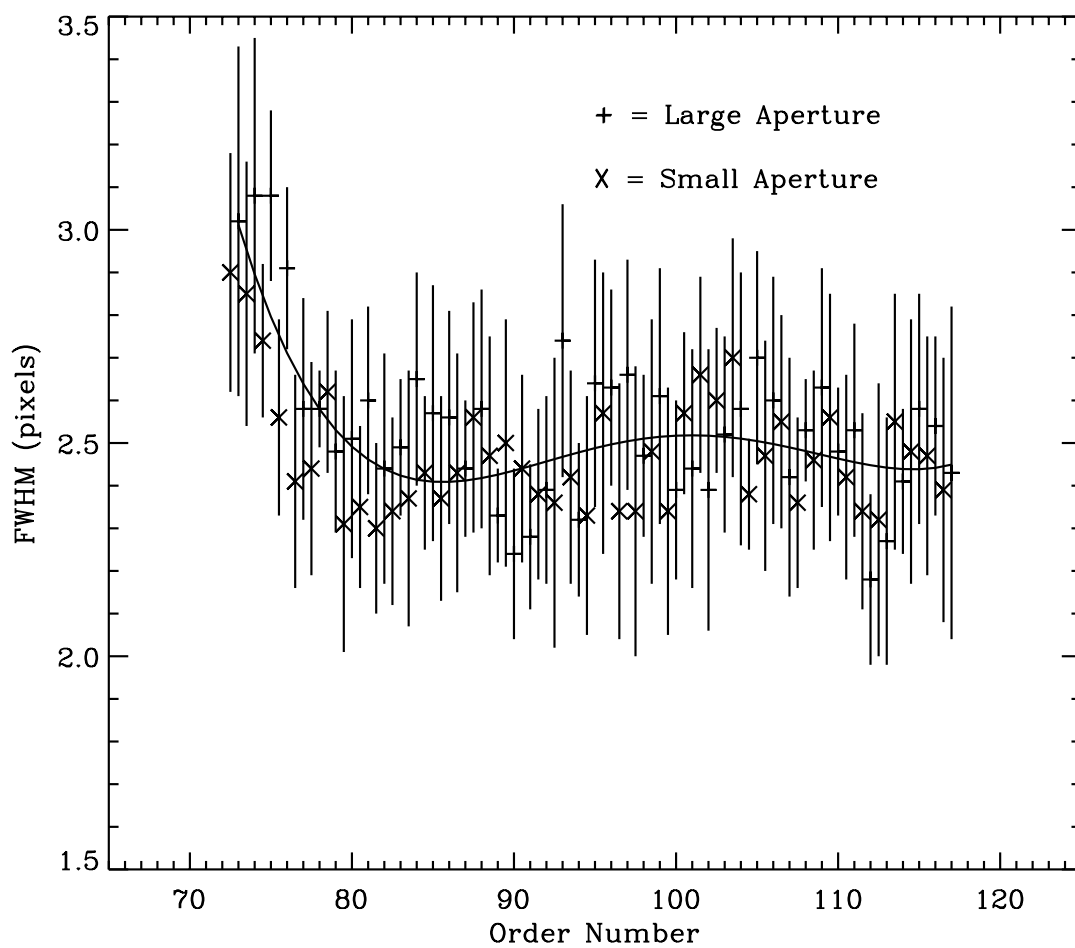


Figure 2.33: LWR high-dispersion spatial resolution for sample position 134. Small-aperture data is horizontally offset to the left of the large-aperture data by half an order.

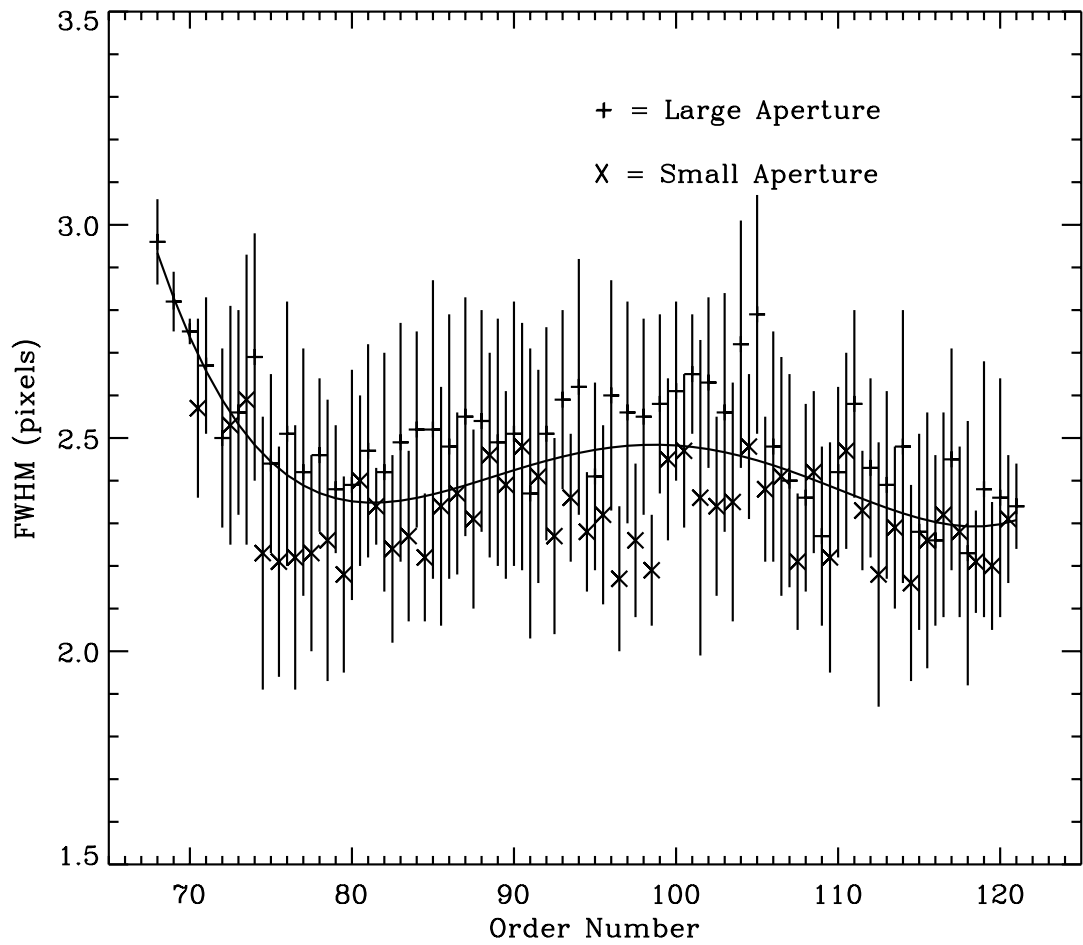


Figure 2.34: LWR high-dispersion spatial resolution for sample position 258. Small-aperture data is horizontally offset to the left of the large-aperture data by half an order.

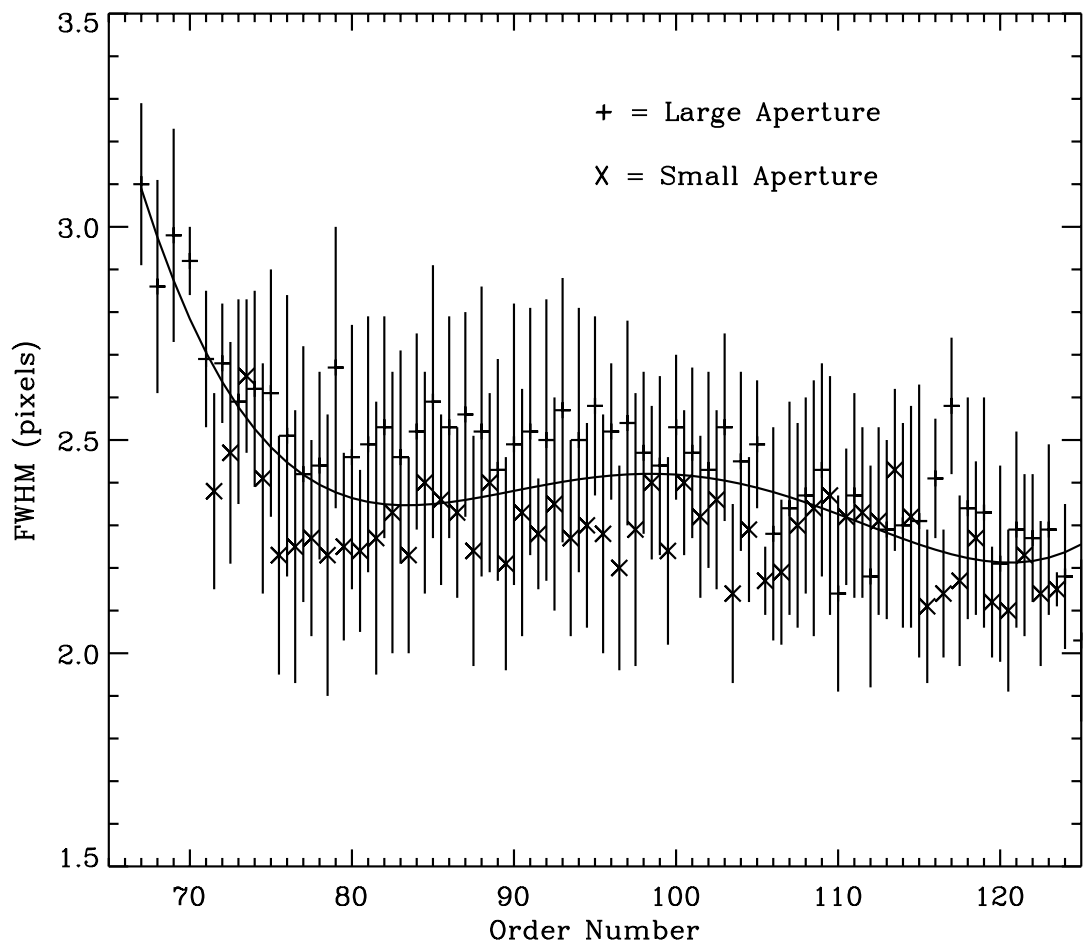


Figure 2.35: LWR high-dispersion spatial resolution for sample position 384. Small-aperture data is horizontally offset to the left of the large-aperture data by half an order.

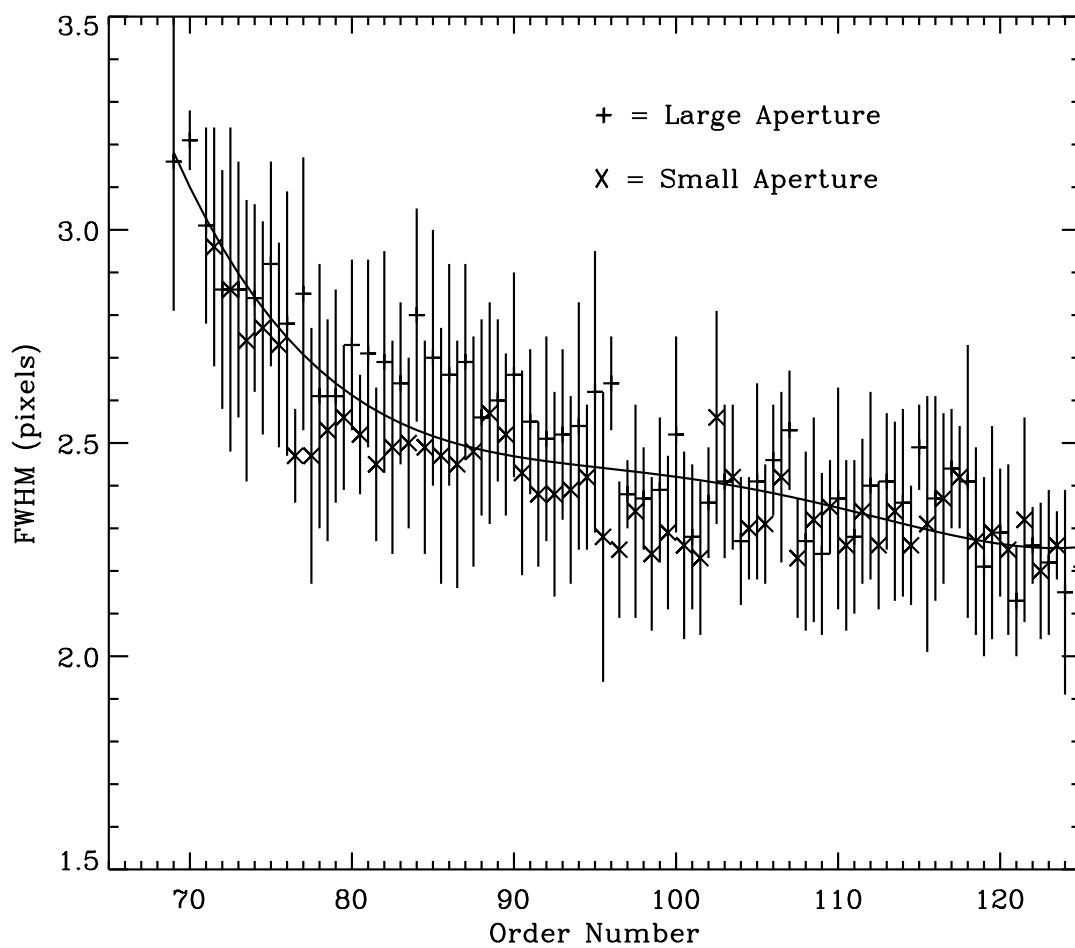


Figure 2.36: LWR high-dispersion spatial resolution for sample position 507. Small-aperture data is horizontally offset to the left of the large-aperture data by half an order.

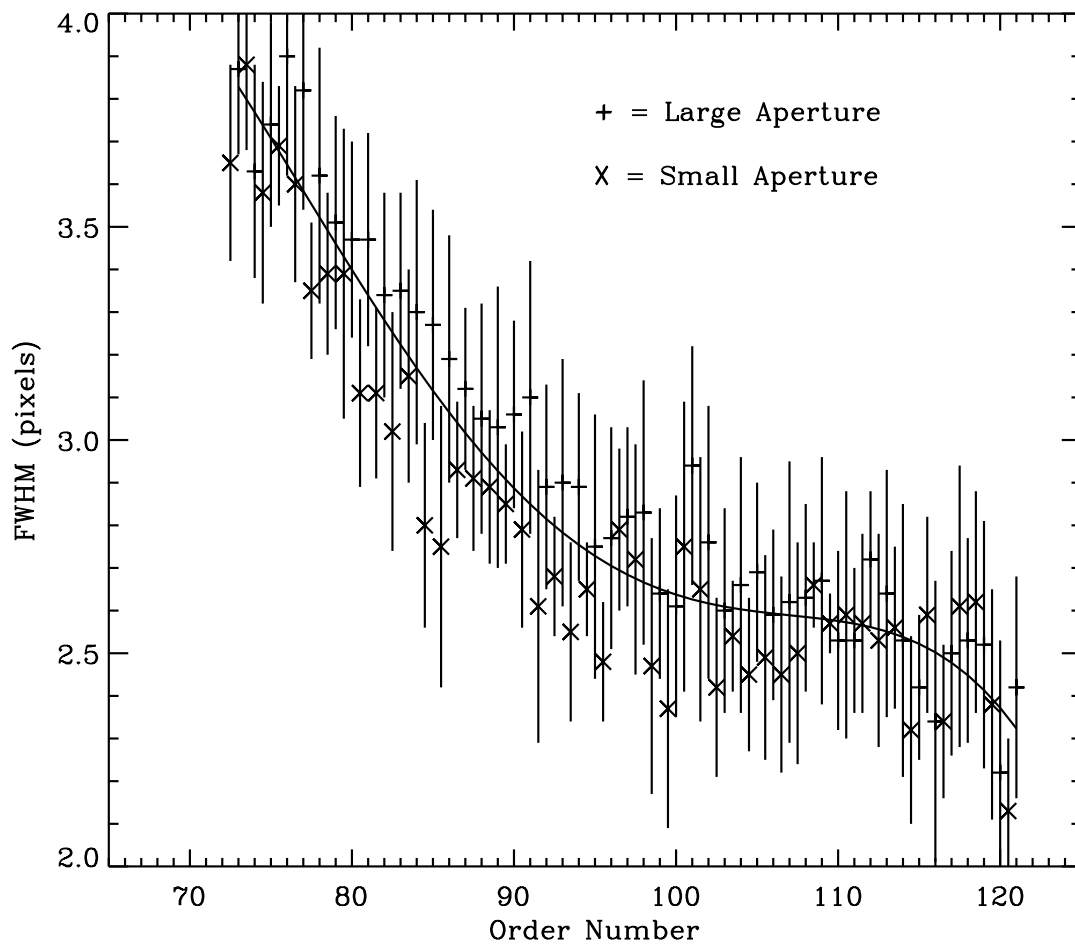


Figure 2.37: LWR high-dispersion spatial resolution for sample position 615. Small-aperture data is horizontally offset to the left of the large-aperture data by half an order.

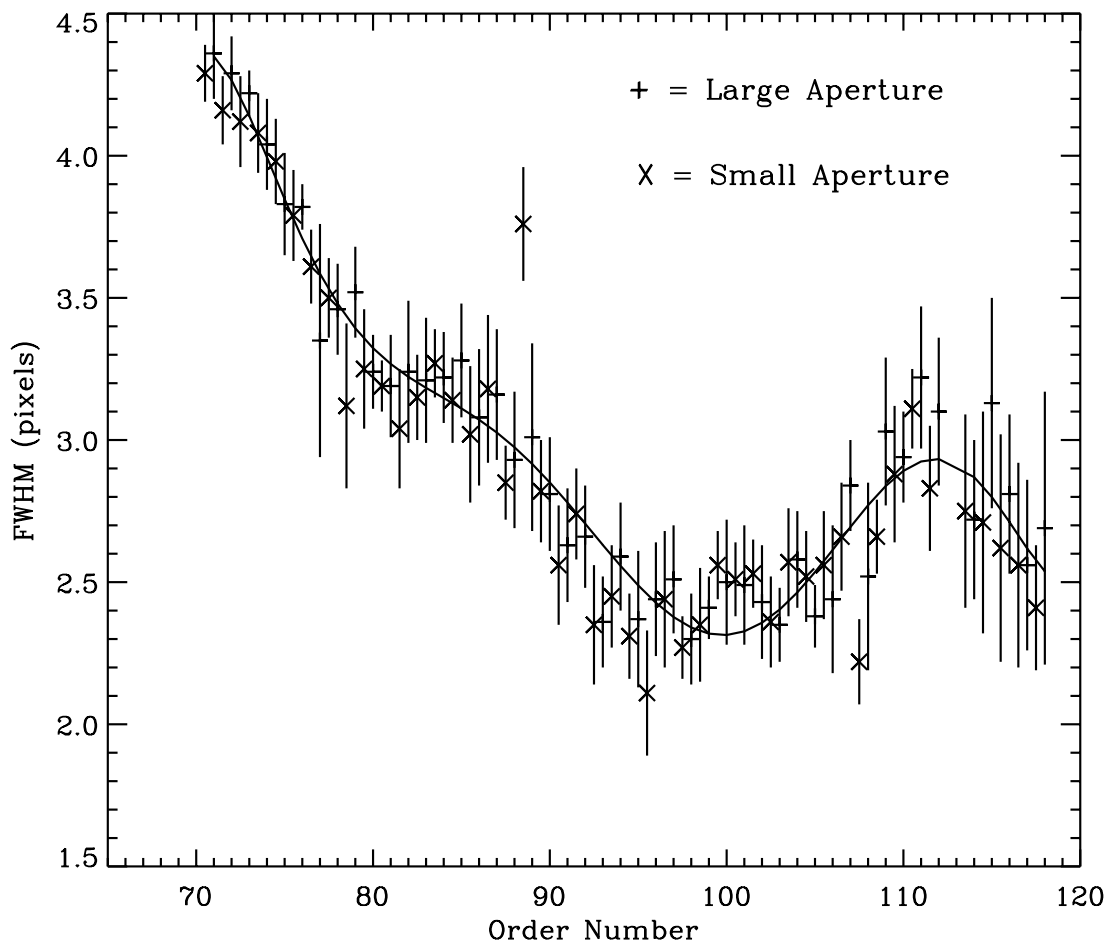


Figure 2.38: SWP high-dispersion spatial resolution for sample position 134. Small-aperture data is horizontally offset to the left of the large-aperture data by half an order.

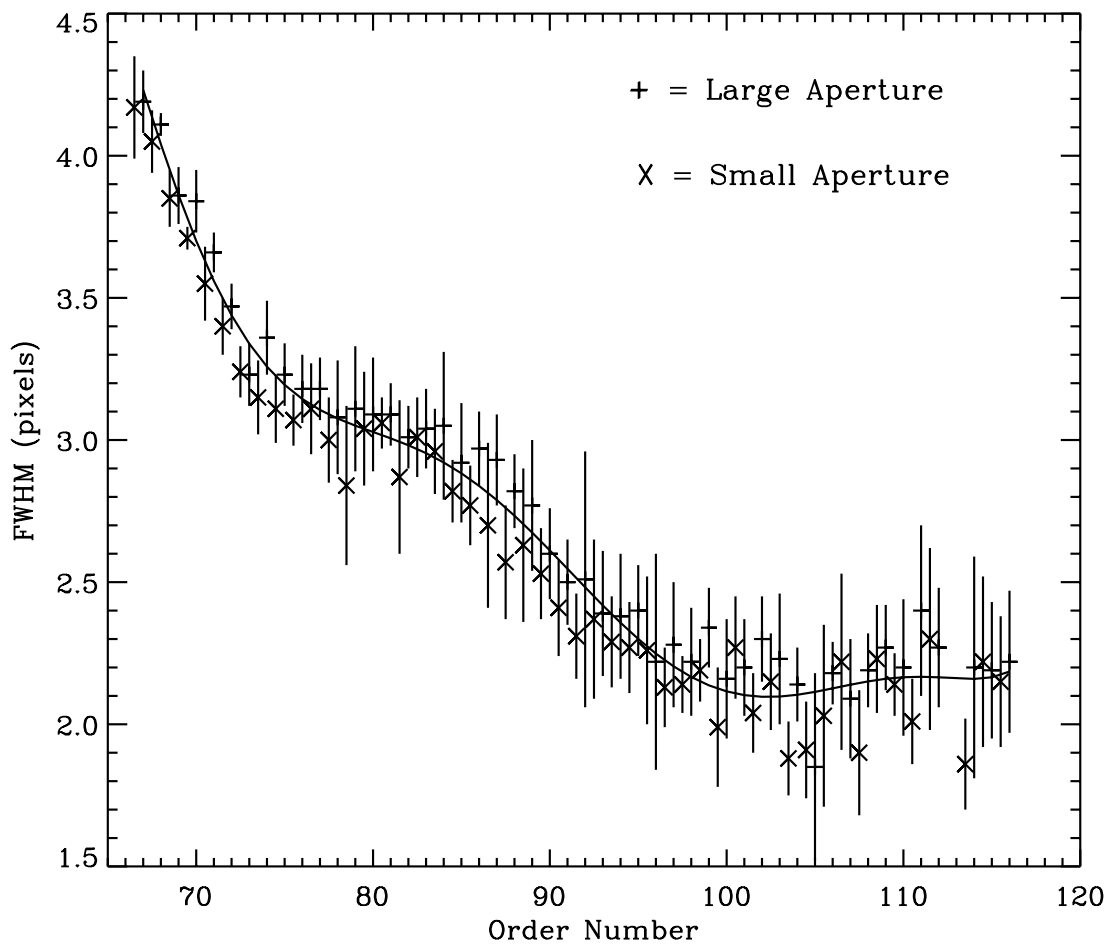


Figure 2.39: SWP high-dispersion spatial resolution for sample position 258. Small-aperture data is horizontally offset to the left of the large-aperture data by half an order.

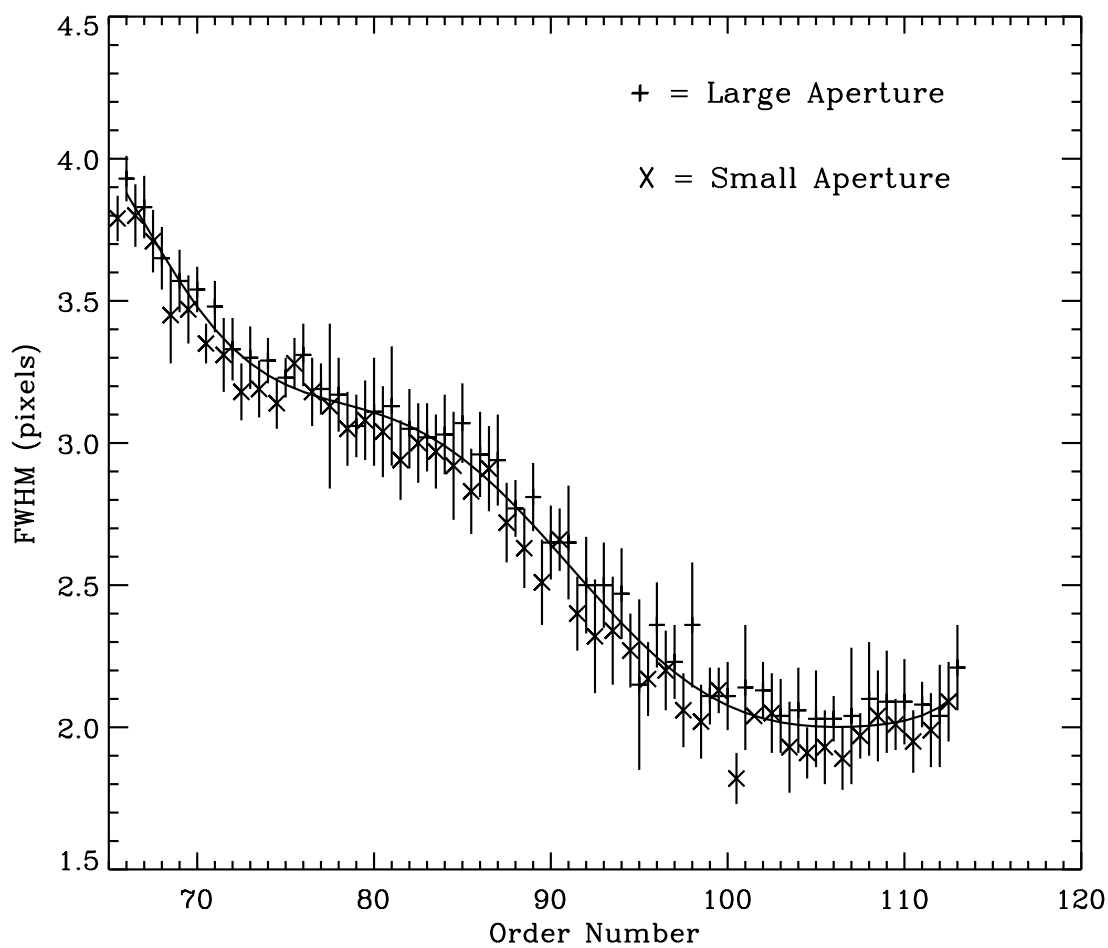


Figure 2.40: SWP high-dispersion spatial resolution for sample position 384. Small-aperture data is horizontally offset to the left of the large-aperture data by half an order.

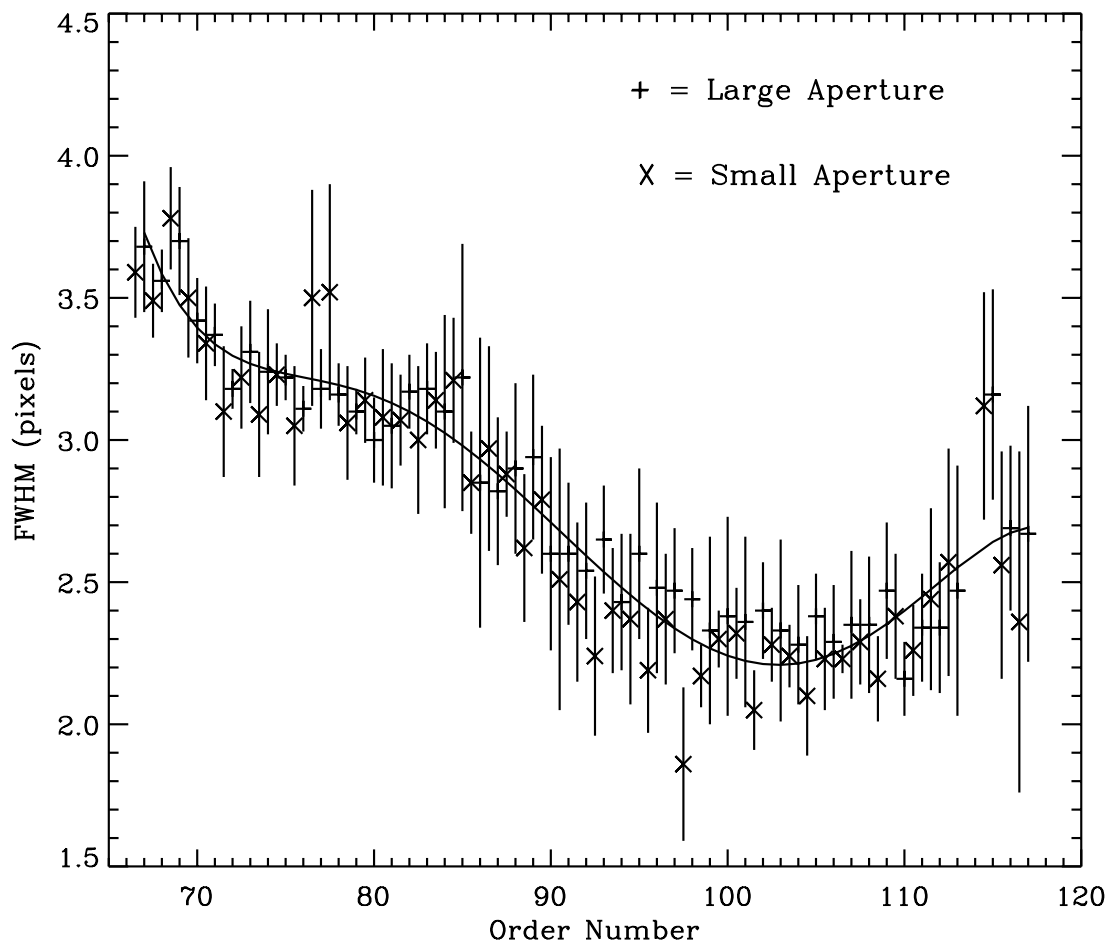


Figure 2.41: SWP high-dispersion spatial resolution for sample position 507. Small-aperture data is horizontally offset to the left of the large-aperture data by half an order.

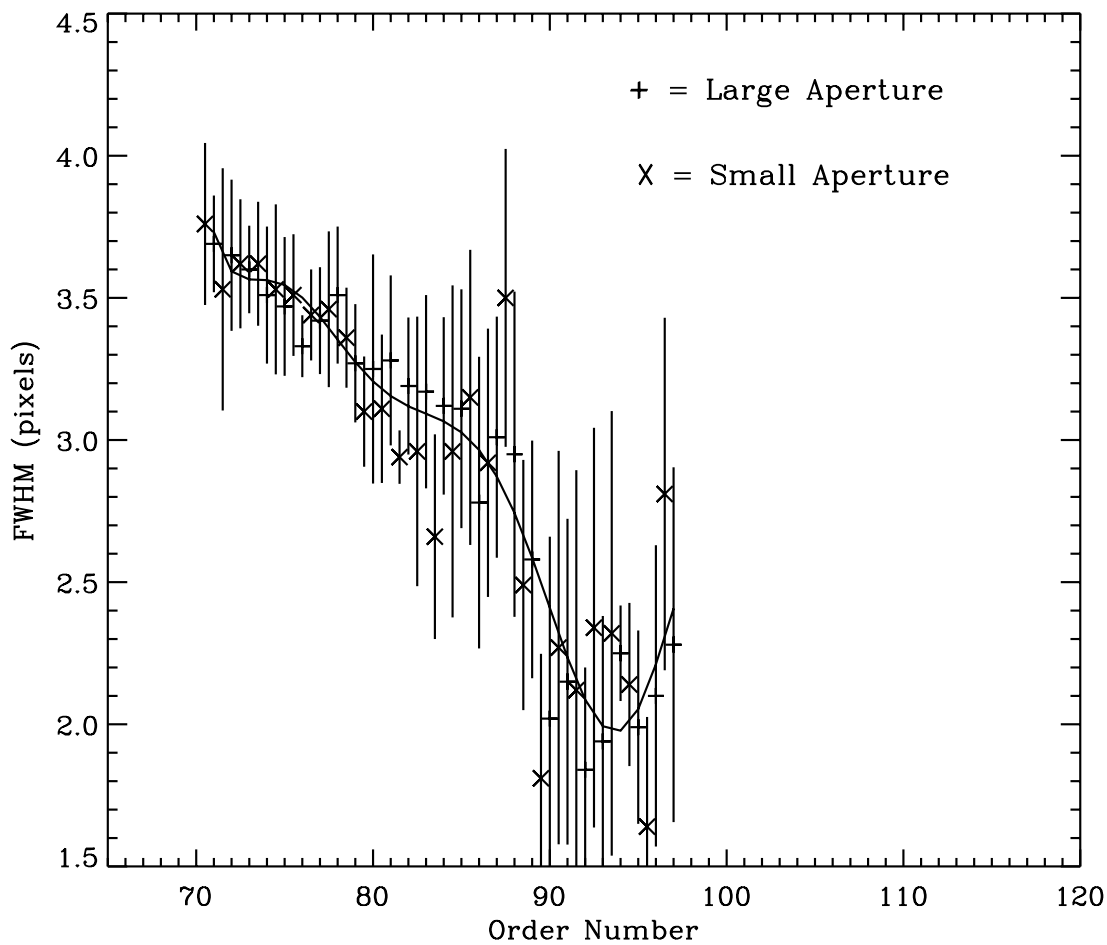


Figure 2.42: SWP high-dispersion spatial resolution for sample position 615. Small-aperture data is horizontally offset to the left of the large-aperture data by half an order.